DEPARTMENT OF THE INTERIOR

U.S. GEOLOGICAL SURVEY

In-Situ Stress Project
Technical Report Number 2:
Televiewer Data Report for the Test Interval 6250-6935 ft, Cajon Pass Well, California

by

James E. Springer and Mark J. Ader

Open-File Report 87-290

Menlo Park, California

1987

CONTENTS

TABLES

FIGURES

UNITED STATES
DEPARTMENT OF THE INTERIOR
GEOLOGICAL SURVEY

TELEVIEWER DATA REPORT FOR THE TEST INTERVAL 6250-6935 FT, CAJON PASS WELL, CALIFORNIA

James Springer and Mark Ader

ABSTRACT

Four borehole televiewer logs were run in the Cajon Pass well, covering the test interval from 6250 ft to 6935 ft (1905 to 2114 m). The best image resolution was in the interval from 6711 to 6935 ft (2046 to 2114 m) where the drill bit size was 6-1/2 inches (16.5 cm). Above that section, the bit size was 8-1/2 inches (21.6 cm), and the tool was poorly centralized, resulting in lower resolution. Depth uncertainties were checked and adjusted using the drillers depths for the bottom of the casing at 6000 ft (1829 m), the hole size change at 6711 ft (2046 m), and fractures that correlated with those on the core at 6748 ft and 6515 ft (2057 and 1986 m).

Few natural fractures were visible on the televiewer logs and most of them had low to moderate dips. Most fractures on the core were closed or filled, causing them to be more difficult to detect on the televiewer logs. The filling material was chlorite and a white fibrose zeolite (?). One fracture offset a gneissic layer 25 mm in a reverse sense.

Twenty-one borehole breakouts were logged for a total of 127 ft (39 m). The average orientation of the breakouts was N5W and the standard deviation was 11 degrees. Hydraulic fractures produced during in-situ stress measurements are visible on the logs and confirm that the maximum horizontal compressive stress is perpendicular to the breakout direction. This maximum stress is parallel to the average trend of the Cleghorn fault and is consistent with a normal component of movement on it. This direction however, is rotated 35 degrees clockwise from that reported in the section from 6000 to 6250 ft (1829 to 1905 m). Further drilling and logging is needed to determine whether this direction continues with depth or is just a localized phenomenon.

INTRODUCTION

During the second phase of the Cajon Pass drilling experiment, an 8-1/2 inch- (21.6 cm) diameter hole was drilled and cored from the casing at 6000 ft to 6711 ft (1829 m to 2046 m) and a 6-1/2 inch (16.5 cm) hole was drilled and cored to 6935

ft (2114 m). This enlarged the diameter of the previous 6000-6250 ft (1829-1905 m) test interval that was reported on by Ader and Springer (1987, Technical Report #1). In order to characterize the new section of open hole, four televiewer logs were run; two before the hydrofrac experiments were carried out and two afterwards. This report describes the televiewer logs and the core and provides a preliminary interpretation of the data.

The BHTV (Zemanek, et al., 1970) is an ultrasonic logging tool that scans the inside of the hole. It is capable of showing fractures that intersect the borehole, holes and washouts in the well, and stress-induced borehole breakouts (Zoback et al., 1985; Plumb and Hickman, 1985).

Seven cores (Table 1) were cut in the new test interval. These cores were collected and cataloged by the USGS. The cores were inspected in order to locate any fractures or veins which might show up on the televiewer log.

TABLE 1
Recovered Core

Core No.	Depth Interval (feet)	Recovered (feet)	Percent Recovered
27	6500-6502.3	2.3	100
28	6502.3-6510	6.2	78
29	6510-6517	7	100
30	6700-6711	8.8	80
31	6740-6755	14.3	95
32	6810-6813	no recovery	0
33	6813-6823	9.3	93
34	6824-6838	6.1	44

The first part of this report presents the borehole televiewer data and describes fractures, breakouts, and the condition of the well. The core is then described and tentative correlations are made between features on the core and features on the televiewer records.

TELEVIEWER LOG

The BHTV information was recorded on black and white polaroid pictures which represent the inside of the hole as if it

were split down the middle along the magnetic north azimuth and laid flat. The brightness on each picture is a function of the amplitude of the reflected pulse. The left and right sides of each image are magnetic north and the directions are clockwise from left to right on the picture; that is north, east, south, west, and north. Planar features, such as fractures, show up as dark sinusoidal traces on the pictures (Zemanek, et al., 1970). Paired dark bands which appear 180 degrees apart are probable borehole breakouts.

The depth reference for the televiewer logs is ground level, located 32 ft (9.8 m) below the drill rig floor. The first log (log 1) was run from 6508 ft to 6938 ft (1984 m to 2115 m) on March 28, 1987. Log 2 was run from 6704 ft to 6899 ft (2044 m to 2103 m) on March 31, 1987 after running an impression packer at 6732 ft (2052 m). Two more logs were run on April 6, 1987. Log 3 was run from 6182 ft to 6918 ft (1885 m to 2109 m) and log 4 was run from 6688 ft to 6923 ft (2039 m to 2111 m). The best images from the 8-1/2 inch section are presented in Appendix A. The best pre- and post-hydrofracturing images from the 6-1/2 inch section are presented in Appendix B.

Problems were encountered with the depth counter on the wireline hoist. This caused depth misties of from 3 to 13 feet (0.9 to 4 m). The depths were compared to features of known depth and then corrected. Features that could be identified are the bottom of the casing at 6000 ft (from wireline trips), the hole size change (6711 ft), and fractures in two of the cores. In the case of log 3, a correct depth reference could be made from overlap with logs of the previous test interval (Ader and Springer, 1987, Technical Report #1). The depths given in Appendix A and B are corrected depths.

Relatively few fractures were visible on the BHTV logs, although one densely fractured zone was encountered from 6335 ft to 6381 ft (1931 m to 1945 m). Most of the natural fractures had low to moderate dip angles similar to those reported from the previous test interval (Ader and Springer, 1987, Technical Report #1).

Borehole Breakouts

Stress-induced borehole breakouts (Bell and Gough, 1979; Zoback, et al., 1985) result from stress distributions around a vertical hole in a non-uniform stress field. Breakouts cause the hole to become elongated in the direction of minimum horizontal in-situ stress. On a televiewer log, breakouts appear as paired vertical dark bands that are 180 degrees apart. Similar dark bands can be caused by a "shadow" effect from an off-centered logging sonde in an otherwise circular hole (see Taylor, 1983). We believe that the dark bands in these televiewer pictures are breakouts for the following reasons: 1) The bands have a consistent orientation throughout this test interval. 2) The bands appear in different logs run with tools having different stiffnesses of centralizer springs. 3) "Shadows" from tool

eccentricity appear on some sections of the log and are not 180 degrees apart. The probable breakouts appear as "holes" superimposed on them. 4) Hydraulically induced fractures from the in-situ stress measurements, as will be discussed below, appear 90 degrees from the breakouts.

Twenty-one breakouts were logged for a total of 127 feet (39 m). These are shown in Table 2. From 6250 to 6711 ft (1905 to 2046 m) where the bit size was larger, 23 ft (7 m) or 5 percent of the hole had breakouts that were visible on the field logs. From 6711 to 6935 ft (2046 to 2114 m), 104 ft (32 m) or 46% of the hole had breakouts logged in it.

TABLE 2
List of Breakouts

Depth Interval (Feet)	Length (Feet)	Average Azimuth (True)
6704-6705	1	165
6690-6693	3	178
6685-6688	3	170
6639-6640	1	160
6628-6634	6	180
6612-6614	2	183
6528-6531	3	175
6447-6449	2	180
6425-6427	2	180
6930-6935	5	160
6915-6927	12	172
6907-6913	6	178
6902-6904	2	193
6897-6900	3	188
6888-6894	6	173
6855-6856	1	165
6834-6838	4	155
6797-6808	11	193
6764-6794	30	192
6757-6761	4	158
6735-6755	20	175

The breakout orientations were plotted on histograms (figs. 1 and 2). In fig. 1, the number of breakouts was plotted as a function of azimuth. In fig. 2, the length of hole affected by breakouts were plotted as a function of azimuth. The mean orientation was N6W and the standard deviation was 11 degrees. When the data are weighted according to the length of hole affected by breakouts, the mean orientation is N5W. When the data are combined with that from the interval from 6000 ft to 6250 ft (1829 m to 1905 m) (Ader and Springer, 1987), the resulting histograms show bimodal distributions (figs. 3 and 4).

This orientation implies that the maximum horizontal stress is oriented N84-85E which is rotated 35 degrees clockwise from

Fig. 1. Breakout frequency vs azimuth.

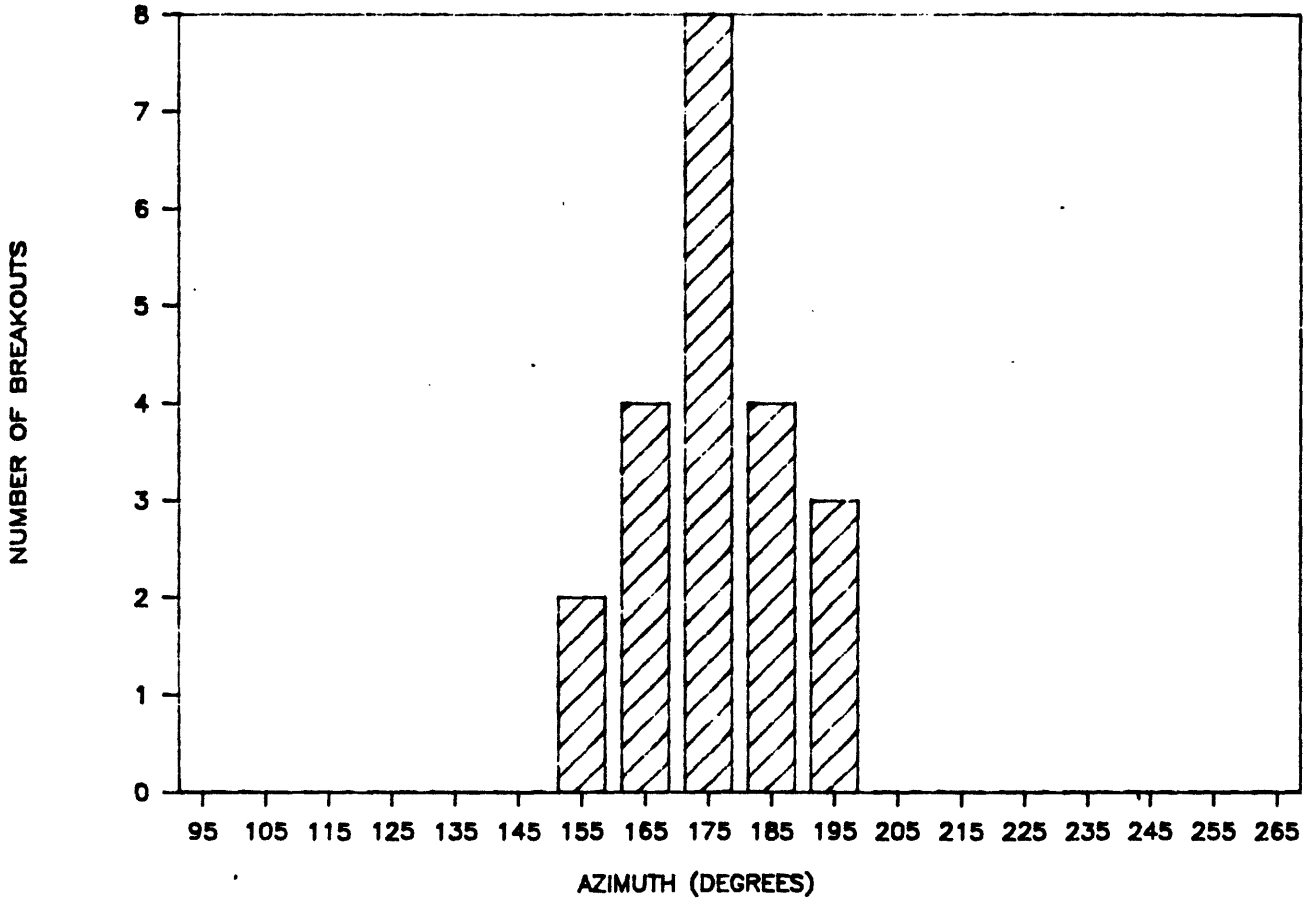

Fig. 2. Breakout length vs azimuth.

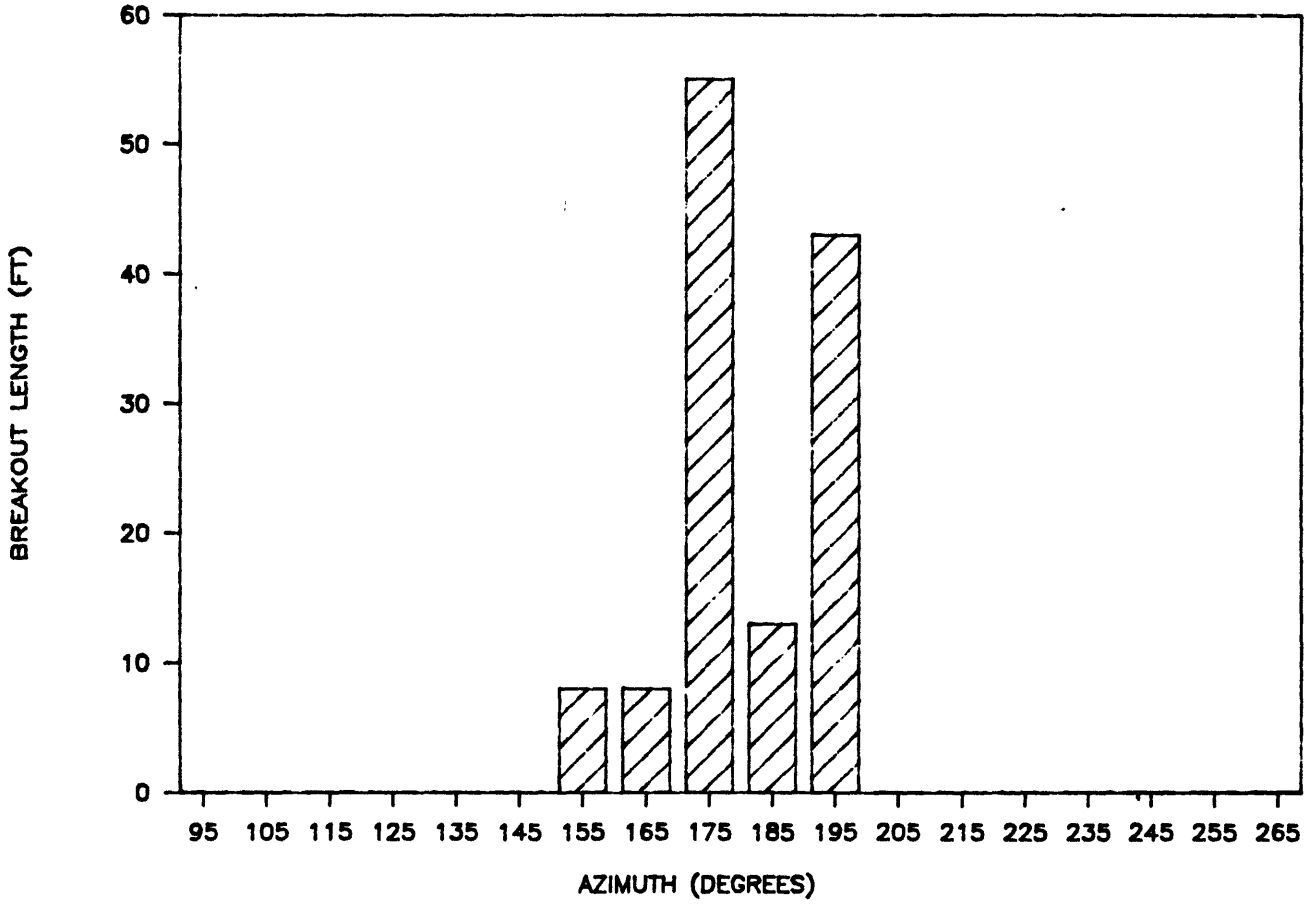

Fig. 3. Breakout frequency vs azimuth

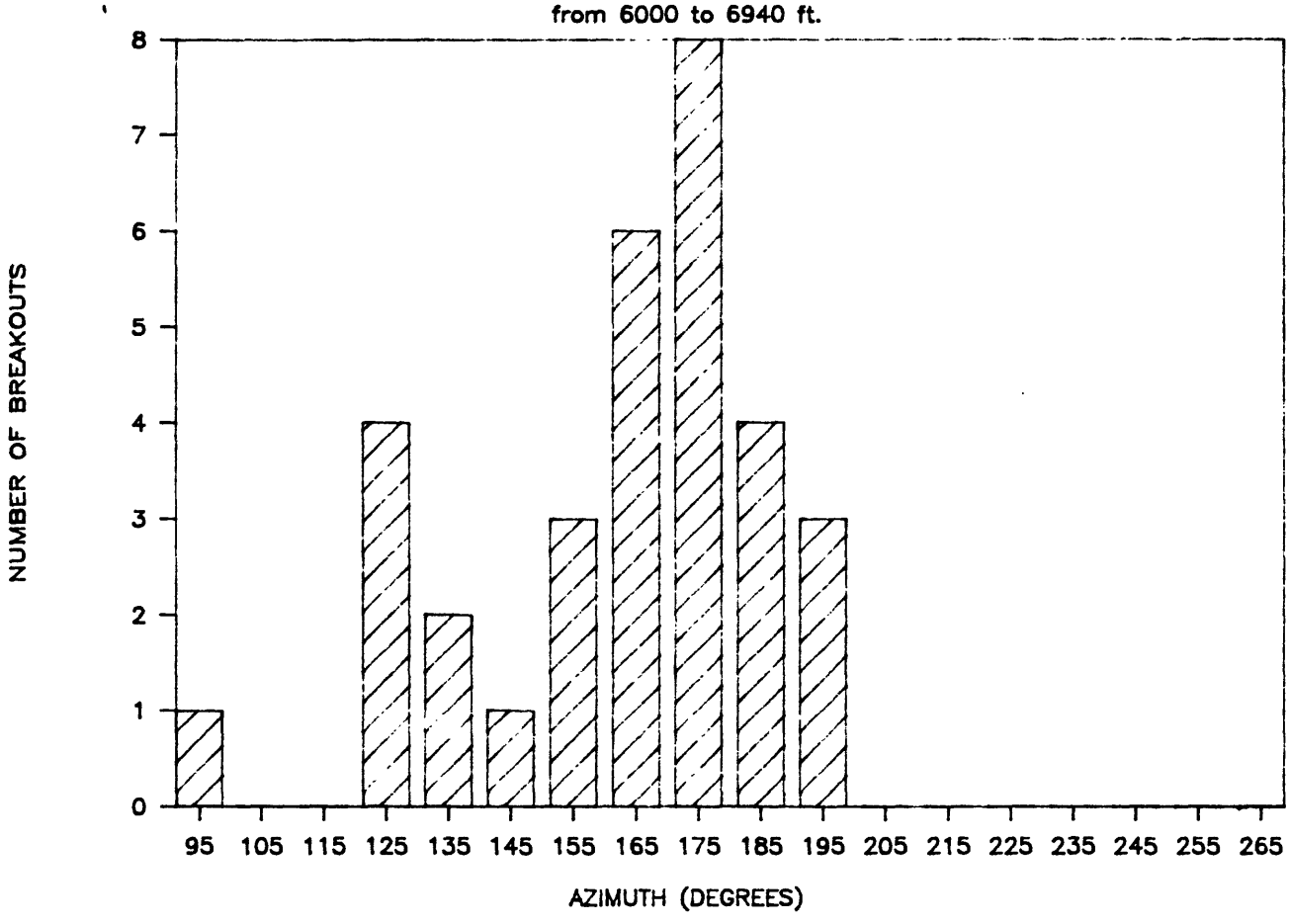

Fig. 4. Breakout length vs azimuth

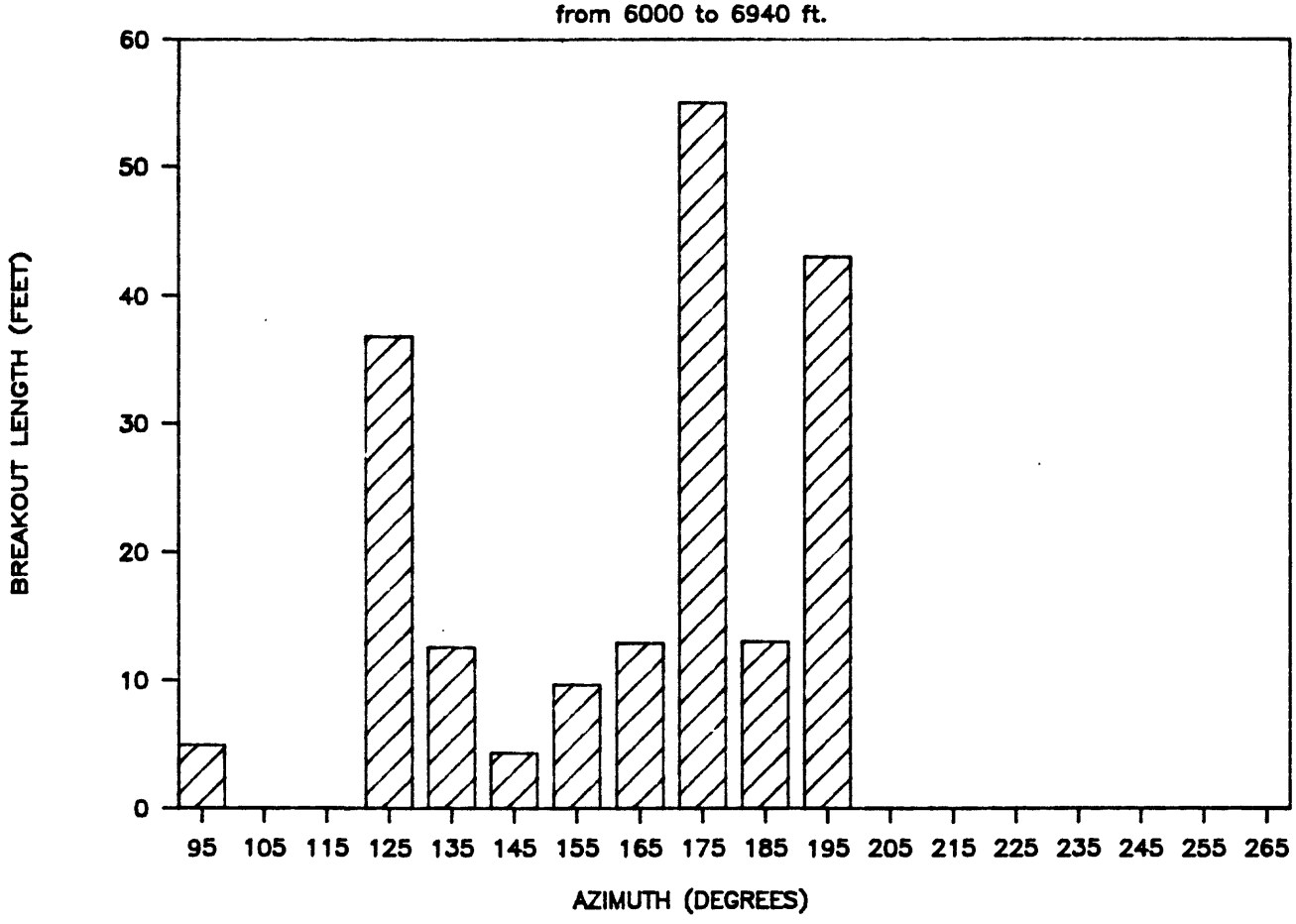

the orientation in the first test interval (6000-6250 ft, see Ader and Springer, 1987). Plotting the maximum horizontal stress direction derived from the breakouts as a function of depth (fig. 5) shows the change. Where the log coverage overlaps with that from the previous test interval, the breakout orientations are the same, indicating that the change is real and not an artifact of the imaging process.

Comparison of Pre-fracturing and Post-fracturing Logs

Hydraulically induced fractures can be seen in two of the test intervals on the post-frac televiewer logs (Appendix B). The interval depths and fracture orientations are shown in Table 3. The post-frac logs of intervals 4 (6859 ft; 2091 m) and 7 (6716 ft; 2048 m) did not show any visible hydraulic fractures or new breakouts.

In frac interval 5 (6839 ft; 2085 m), the pre-frac log does not show any cracks. The post-frac log shows two vertical cracks, 180 degrees apart between 6829 ft (2082 m) and 6856 ft (2090 m). These fractures extend 8 ft (2.4 m) above the frac interval and 12 ft (3.7 m) below the interval. The average strike of this fracture, after correcting for magnetic declination is N76E-S76W. This is within one standard deviation of the orthogonal to the mean breakout orientation. Two holes, approximately orthogonal to the direction of the vertical cracks are visible within the frac interval on the post-frac log. Two more are visible at 6835 ft (2084 m). These are probably the beginning of breakouts that occurred after the pre-frac log was run. Below the frac interval, incipient breakouts appear on the post-frac log. These extend from 6845 ft to 6856 ft (2087 m to 2090 m) and are characterized by pairs of irregular vertical cracks enclosing the breakout azimuth. These are similar to the incipient breakouts described by Springer et al. (1987) from downhole photographs at the Nevada Test Site.

In frac interval 6 (6732 ft; 2052 m), incipient breakouts, can be seen on the pre-frac log. These show up as vertical cracks close to the breakout directions. One such crack extends from about 6730 ft (2052 m) to the edge of a breakout at 6745 ft (2056 m). In the post-frac log, a well developed breakout is present in the frac interval and 90 degrees from it, a vertical hydraulic fracture can be seen. A rubber impression was taken from this interval, confirming that there was an elongation with a vertical fracture oriented 90 degrees to it.

In the two intervals where hydraulic fractures were visible on the logs, these fractures extended beyond the frac interval. These two intervals also had breakout growth after the first BHTV log. The open fractures and continued spalling may be the result of differences in lithologic character between these sections and the ones where the fractures were not visible.

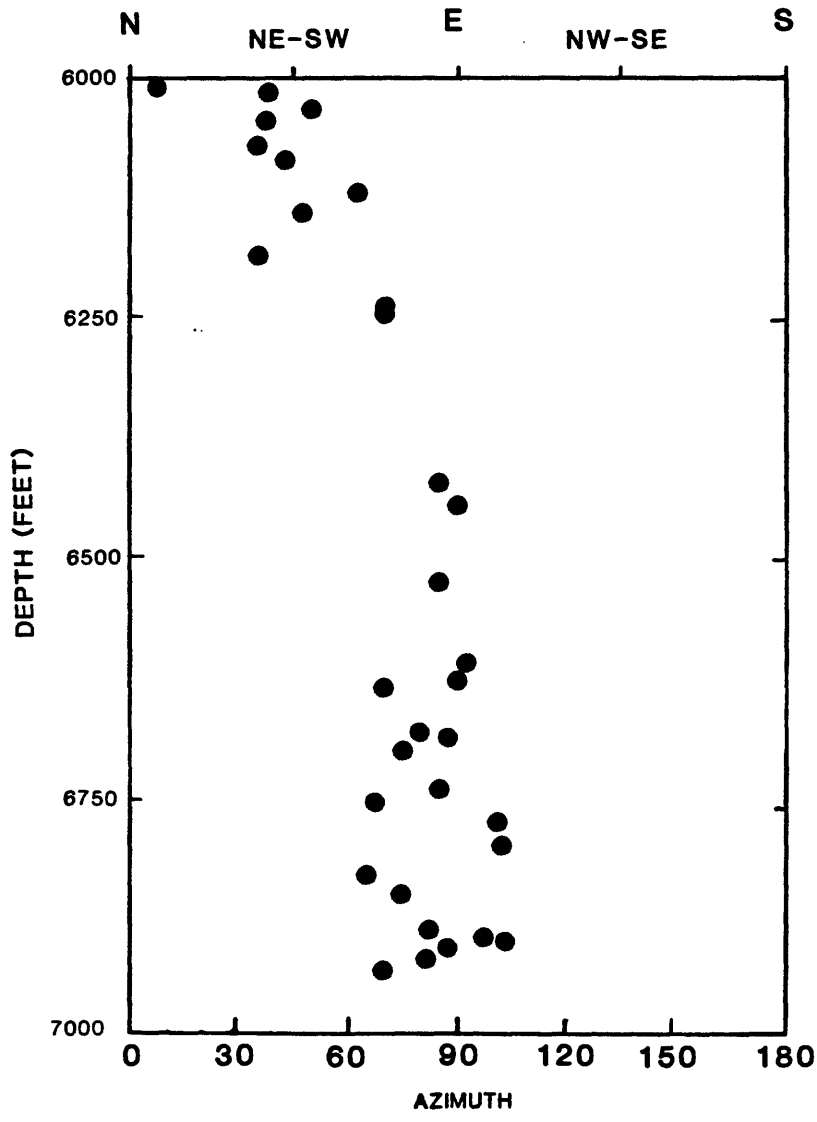

Fig. 5. Azimuth of the maximum horizontal stress vs depth as determined from well bore breakouts.

TABLE 3
Hydraulic Fractures Seen on the Post-Frac Log

Frac No.	Depth (Feet)	Fracture Azimuth (True)
4	6859	Not visible.
5	6839	N76E
6	6732	N81E
7	6716	Not visible.

CORE DESCRIPTION

Core recovery was from zero to 100 percent and averaged 74 percent which was slightly higher than that from the previous test interval (Ader and Springer, 1987). A summary description of the core is presented in Table 4. When assigning depths to the recovered core, the bottom of the core was assigned to the lower depth of the coring interval. In accordance with the driller's record, footages were marked ascending the core. The cores were inspected for fractures and veins that might show up on the televiewer records.

The main mineralization occuring in fractures is a white to clear zeolite (?) having fibers that grow perpendicular to the fractures. The other fracture filling material that occurs in abundance is chlorite. Its habit is fibrose, parallel to the fractures. The two minerals rarely occur together.

Three fractures show evidence of movement. One offsets a gneissic layer 25 mm in a reverse sense and is itself offset by a second one in a left-lateral sense. Another fault has dip-slip slickensides, although the sense of movement is uncertain.

Possible correlations between the BHTV logs and the core occur at 6515 ft (1986 m) and 6748 ft (2057 m). The depths of these features agreed with the corrected televiewer depths to within one foot (0.3 m). The scarcity of correlatable features was due, in part, to the relatively intact nature of the rock and pausity of open fractures. Closed or filled fractures are not as readily visible on BHTV pictures as open ones. In the 8-1/2 inch (21.6 cm) section of the hole, an off-centered logging tool inhibited the resolution of the pictures which makes correlations more difficult.

TABLE 4
Core Log

Depth Interval (Feet)	Description
	CORE 27
6502-6502.3	Fine-grained tonalite or quartz diorite, sometimes gneissic. Lots of disking. BHTV log was badly centralized.
	CORE 28
6502.3-6510	Fine-grained tonalite or quartz diorite, sometimes gneissic. BHTV log was badly centralized.
6508.5-6510	High-angle chloritized joint.
	CORE 29
6510-6517	
6510-6513	Fine-grained quartz diorite or tonalite.
6513-6514	Fine-grained, layered amphibole-rich rock.
6514-6515	Coarse-grained felsic gneiss and quartzite.
6515-6517	Fine-grained quartz diorite or tonalite.
6515	Low-angle fracture. Although BHTV log was badly centralized throughout the core interval, a fracture is visible at this depth.
	CORE 30
6700-6711	Medium to coarse-grained, amphibole-bearing quartz diorite or tonalite. BHTV log is good and shows some breakouts but no fractures. Bottom of core is at hole size change.
6702.5-6704	High-angle quartz-rich vein.
6702.8	Subhorizontal fracture - drilling induced (?).
6703.2	High-angle fracture with zeolite (?).
6707.5	Joint with chlorite.
	CORE 31
6740-6755	Coarse-grained felsic gneiss, fine-grained quartz diorite/tonalite, and fine-grained, layered amphibole-rich rock.
6747.5-6748	Pair of high-angle fractures. Probably correlate with fracture pair visible on post-frac BHTV log.
	CORE 33
6813-6823	Medium to fine-grained tonalite or quartz diorite with occasional felsic layers.
6813.1	Low-angle fracture.
6813.8	Low-angle felsic layer.
6814.1	Low-angle open fracture - probably drilling induced.
6815	Low-angle felsic layer.
6816.4	Low-angle fracture with no mineralization.
6816.6-6817.8	Reverse fault with 25 mm offset.

6817.4-6818.2	Fault with slickensides. Offsets previous fault in a left-lateral sense.
6817.8	Horizontal fracture. No mineralization.
6818.2-6819.3	Multiple fractures with various orientations.
6819.7	Subhorizontal fracture. No mineralization.
6820.1	High-angle fracture with zeolite (?) and gouge.
6820.3	High-angle fracture.
6820.5	High-angle, branching dip-slip fault with chlorite gouge. Sense of movement from slickensides is uncertain.
6821	Multiple fractures with zeolite (?) filling and various orientations.
6821.2	High-angle fracture - no mineralization.
6822	Sub-vertical fracture with zeolite (?) filling.

CORE 34

6924-6938	Fine-grained quartz diorite or tonalite. BHTV log has very large fracture from 6924 to 6929 which is probably responsible for poor core recovery.
6932.6	Horizontal fracture - no mineralization.
6934-3934.7	Vertical fracture with zeolite (?).
6934.7	High-angle fracture with no mineralization.
6936.3	Folded felsic layer in fine-grained gneissic diorite.

DISCUSSION

Faults in the core indicate reverse movement which may be related to late Miocene thrusting on the Squaw Peak fault (Weldon, 1986). Late Quaternary faulting in the vicinity of the well is both normal and strike-slip (Weldon, 1986), indicating an extensional to strike-slip stress regime. The maximum horizontal stress direction, as indicated from breakouts and hydraulic fractures in this test interval, is sub-parallel to the trend of the Cleghorn fault (fig. 6). This fault is an oblique-slip fault with both normal and left-lateral movement on it (Meisling and Weldon, 1982; Weldon, 1986). The stress direction in this section of the well is consistent with the normal motion on it while the direction from the previous interval (Ader and Springer, 1987) is consistent with left-lateral movement.

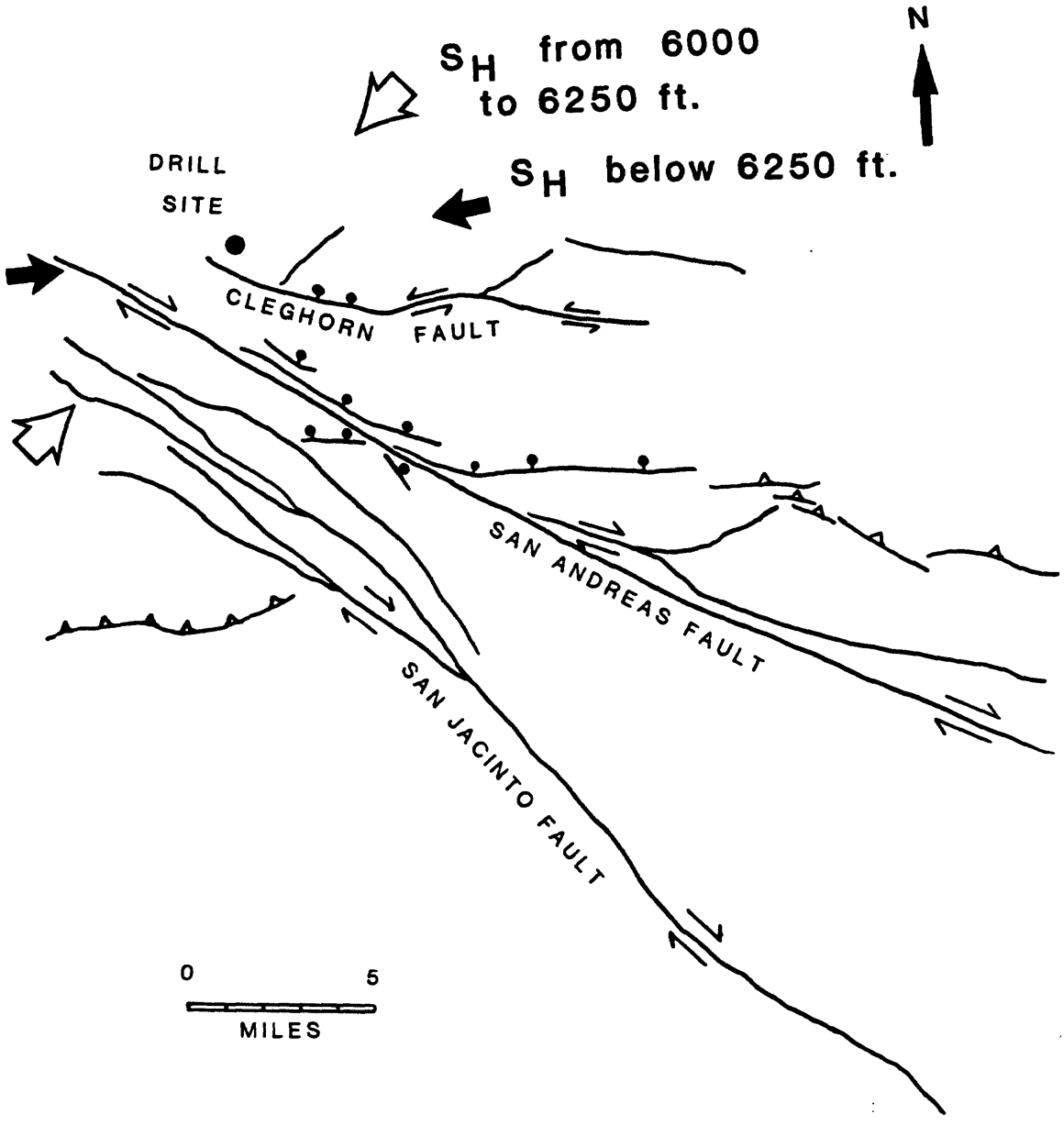

Fig. 6. Generalized fault map of the Cajon Pass area showing the directions of maximum horizontal compressive stress in the drill hole (Map from Weldon, 1986).

Earthquake focal mechanisms within 6 mi (10 km) of the San Andreas fault in the Cajon Pass area are both normal and strike slip (Jones, 1987, in press). Inversion of these focal mechanisms indicate that the major principal stress is vertical and that the maximum horizontal stress is oriented approximately N15W. All of the normal faulting focal mechanisms used by Jones in that study however, were located between the San Andreas and the San Jacinto faults. The breakouts and seismic data suggest that the stress directions are not uniform across the San Andreas fault and that they may change from one fault block to another.

ACKNOWLEDGEMENTS

We thank Jack Healy and Mark Zoback for their encouragement and support of the project and Eric James for helpful discussions and advice. Ray Weldon reviewed the manuscript and made helpful suggestions.

REFERENCES

Ader, M.J. and Springer, J.E., 1987, In-situ stress project, technical report number 1: Televiewer data report for the test interval 6000-6250 ft, Cajon Pass well, California: U.S. Geological Survey, Open-File Report 87-289, 24p.

Bell,J.S. and Gough, D.I., 1979, Northeast-southwest compressive stress in Alberta; Evidence from oil wells: Earth and Planetary Science Letters, v.45, pp.475-482.

Jones, L.M., 1987, Focal mechanisms and the state of stress on the San Andreas fault in southern California: Submitted to Journal of Geophysical Research.

Meisling, K.E. and Weldon, R.J., 1982, Slip-rate, offset, and history of the Cleghorn fault, western San Bernardino Mountains, southern California: Geological Society of America, Abstracts with Programs, v.11, no.3, p.215.

Plumb, R.A. and Hickman, S.H., 1985, Stress-induced borehole elongation: a comparison between the four-arm dipmeter and the borehole televiewer in the Auburn Geothermal Well: Journal of Geophysical Research, v.90, pp.5513-5521.

Stock, J.M., Healy, J.H., and Svitek, J.F., 1986, Hydraulic fracturing stress measurements at Black Butte, Mojave desert, CA: EOS, Transactions, American Geophysical Union, v.67, no.16, p.382.

Springer, J.E., Thorpe, R.K., and McKague, H.L., 1987, Borehole elongation and its relation to tectonic stress at the Nevada Test Site: Submitted to Journal of Geophysical Research.

Taylor, T.J., 1983, Interpretation and application of borehole televiewer surveys: Society of Professional Well Log Analysts, 24th Annual Logging Symposium, paper no. QQ, 19p.

Weldon, R.J., 1986, The late Cenozoic geology of Cajon Pass; Implications for tectonics and sedimentation along the San Andreas fault: Ph.D. Thesis, California Institute of Technology, Pasedena, California, 400p., 12 plates.

Weldon, R.J., Meisling, K.E., Sieh, K.E., and Allen, C.R., 1981, Neotectonics of the Silverwood Lake area, San Bernardino

County: Report to the California Department of Water Resources, 22p., 11 figs., 1 map.
Zemanek,J., Glenn, E.E., Norton, L.J., and Caldwell, R.L., 1970, Formation evaluation by inspection with the borehole televiewer: Geophysics, v.35, no.2, pp.245-269.
Zoback, M.D., Moos, D., Mastin, L.G., and Anderson, R.N., 1985, Well bore breakouts and in-situ stress: Journal of Geophysical Research, v.90, no.B7, pp.5523-5530.

APPENDIX A

TELEVIEWER LOG FROM THE 8-1/2 INCH SECTION OF THE HOLE

8-1/2 INCH HOLE

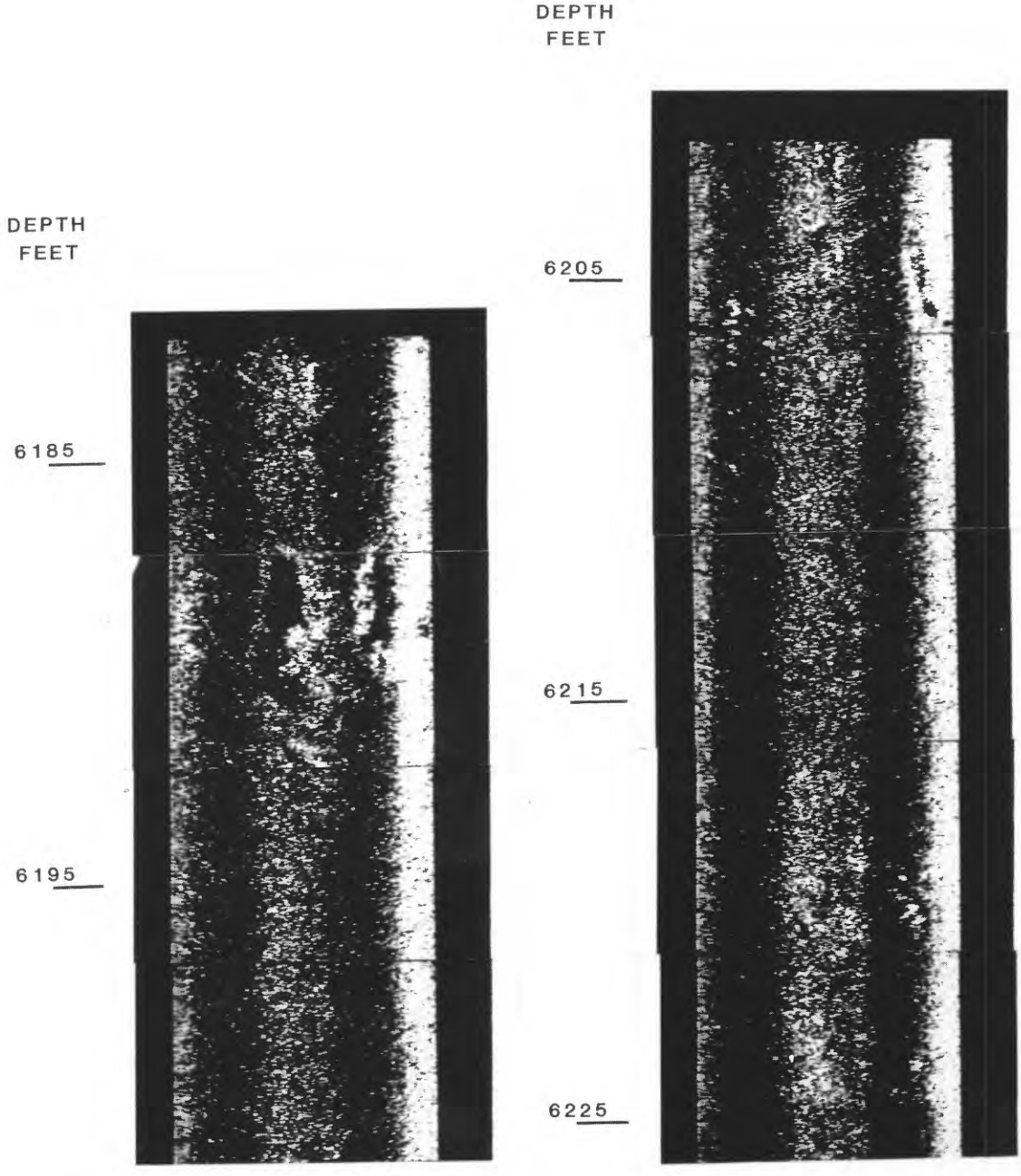

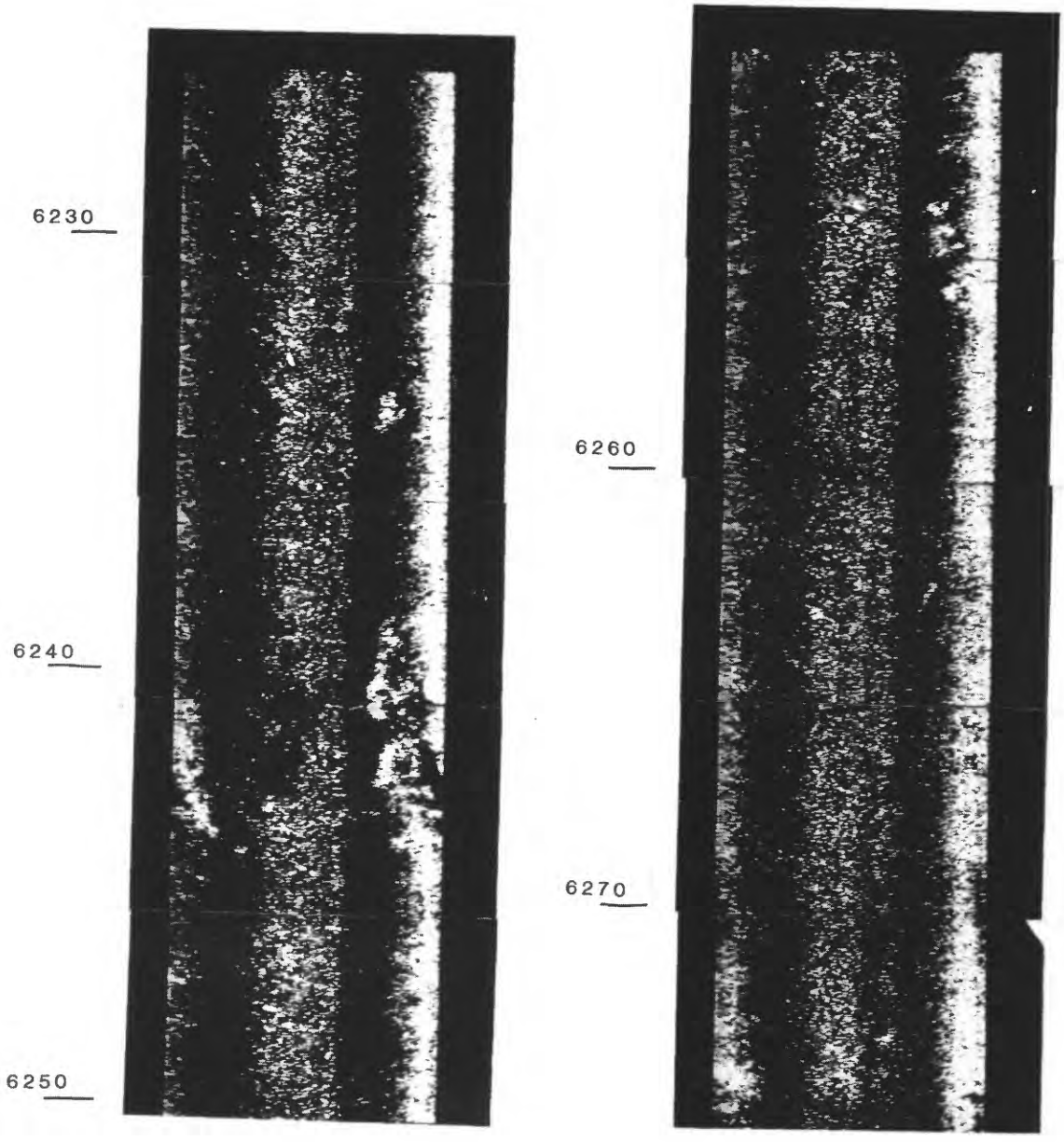
6230
6240
6250
6260
6270

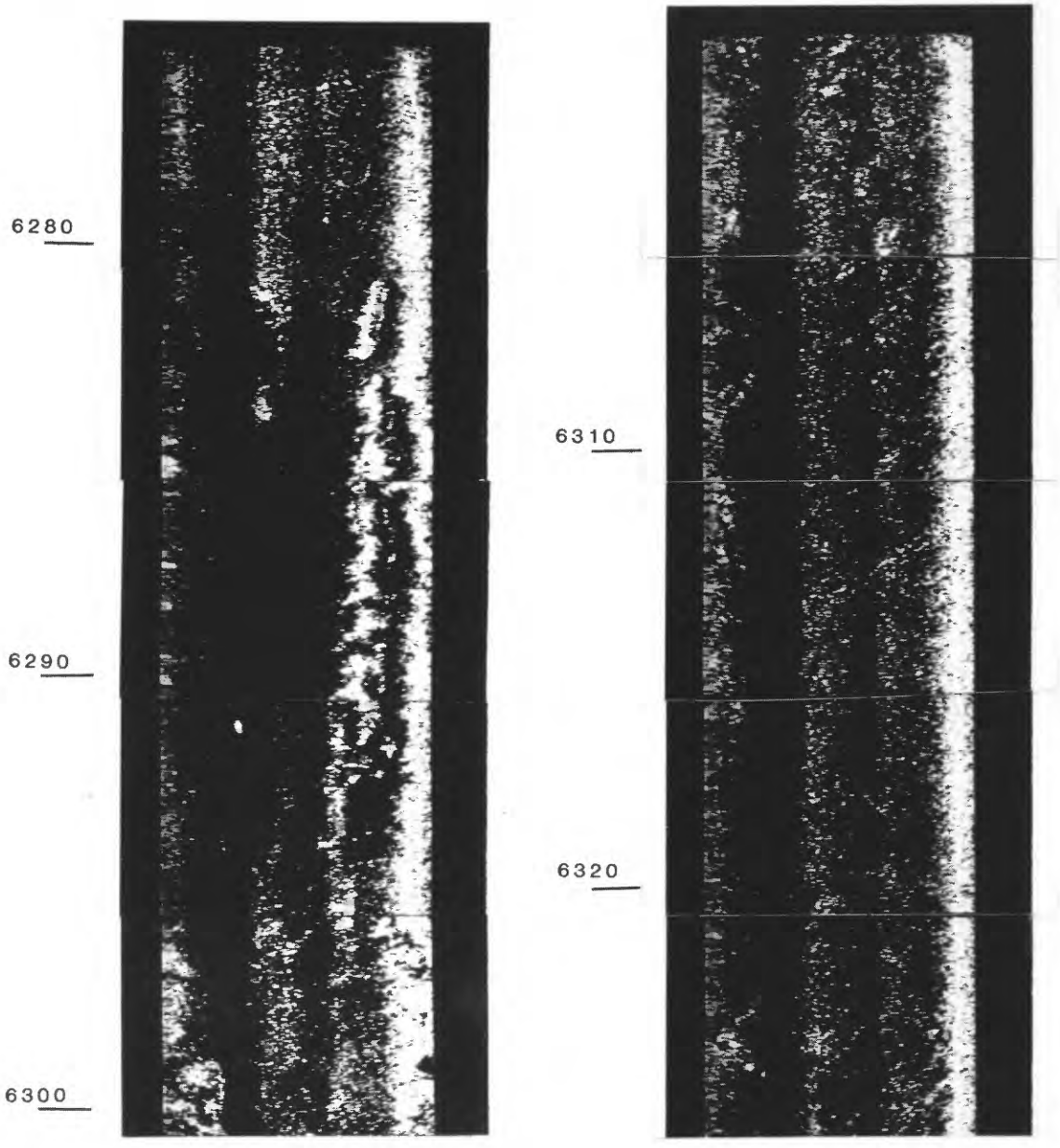
6280
6290
6300
6310
6320

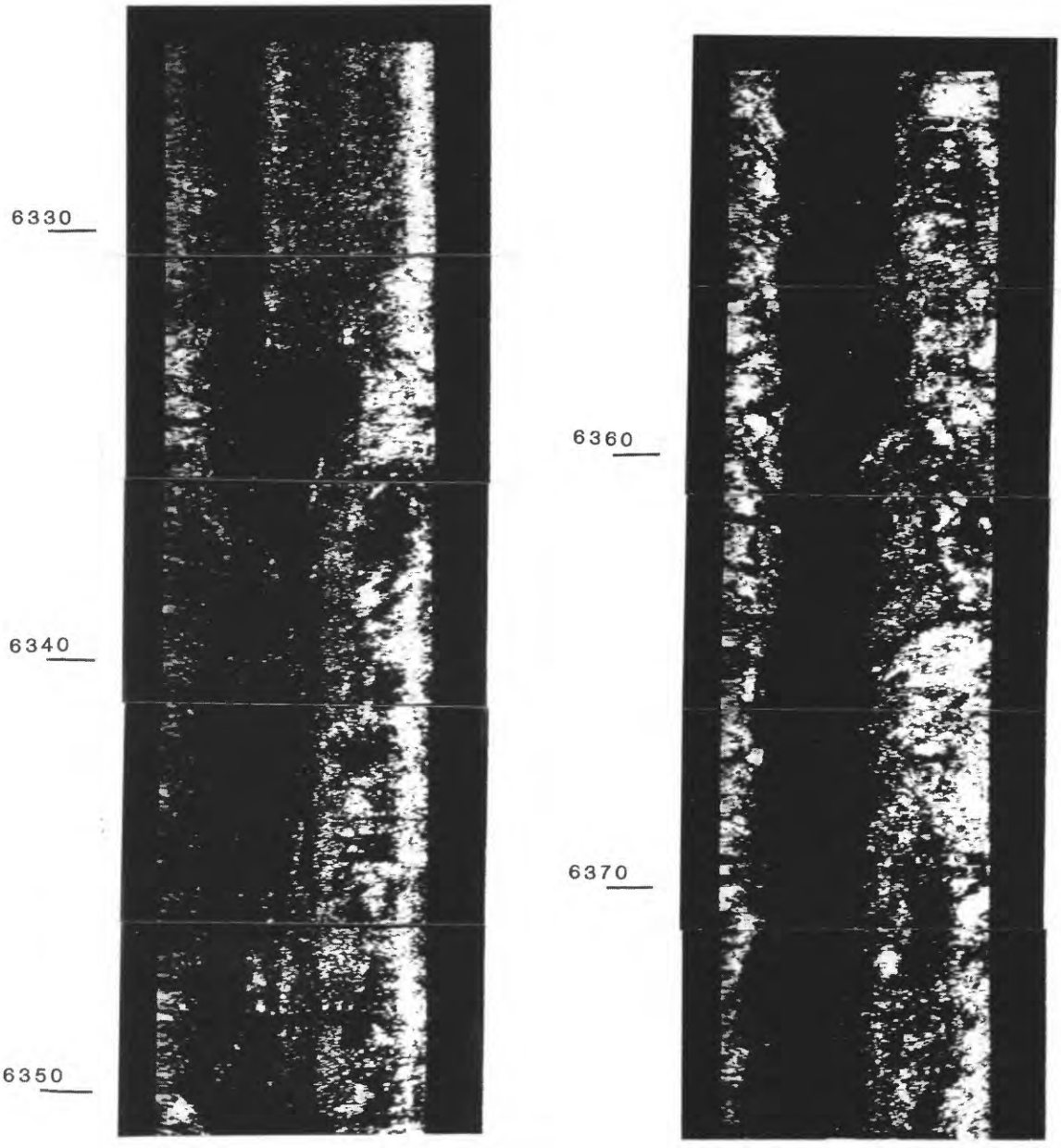
6330
6340
6350
6360
6370

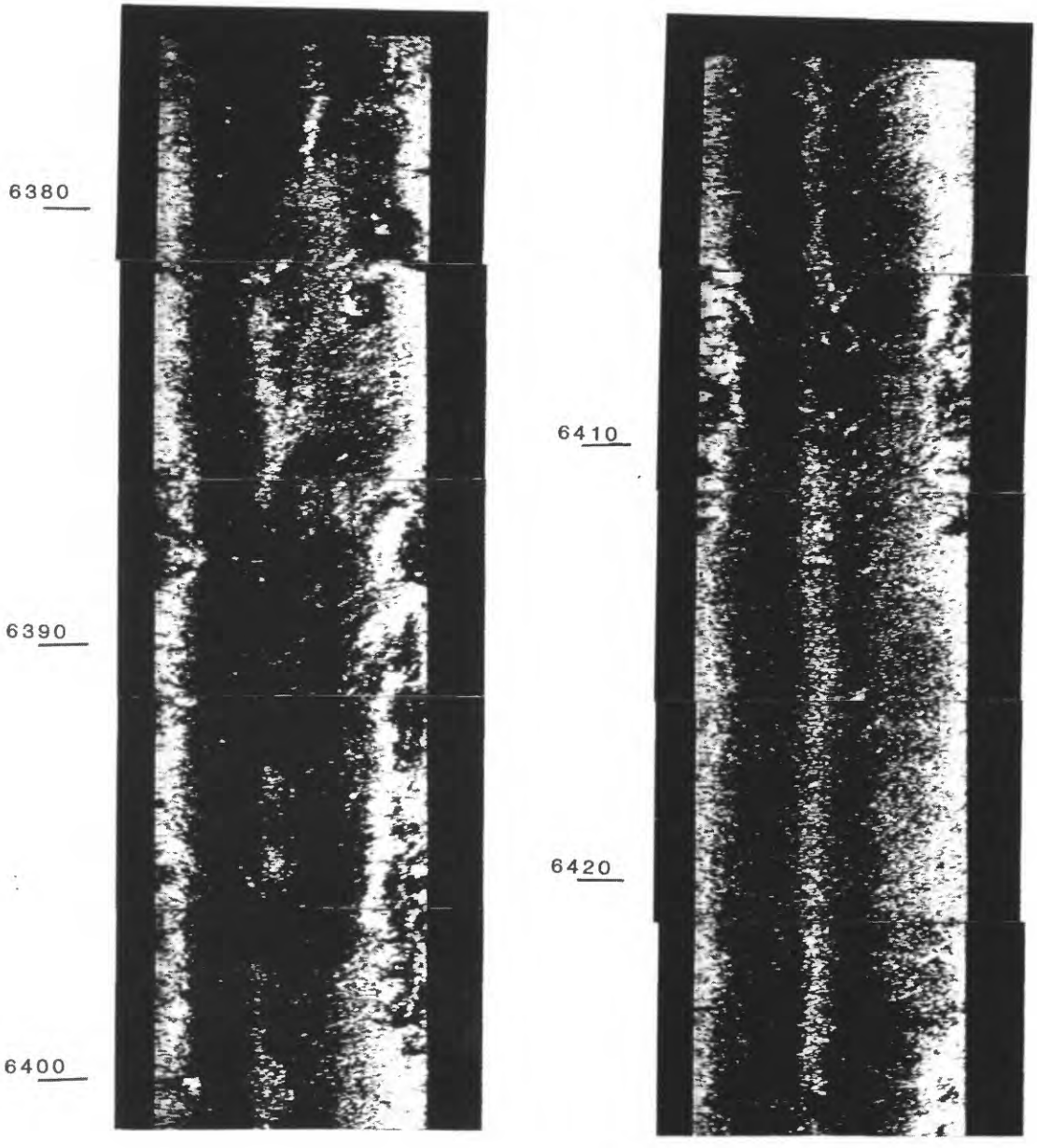
6380
6390
6400
6410
6420

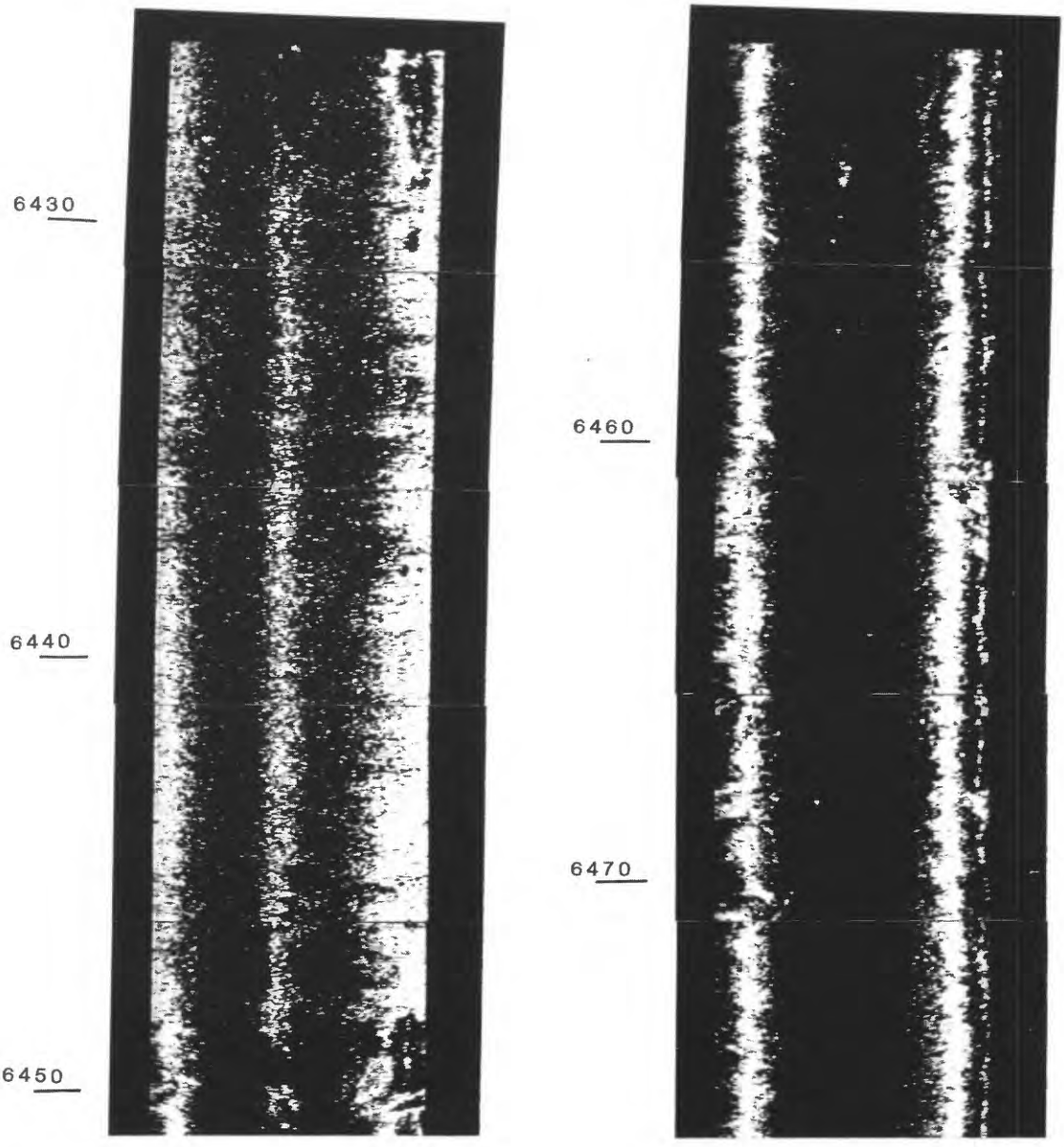
6430
6440
6450
6460
6470

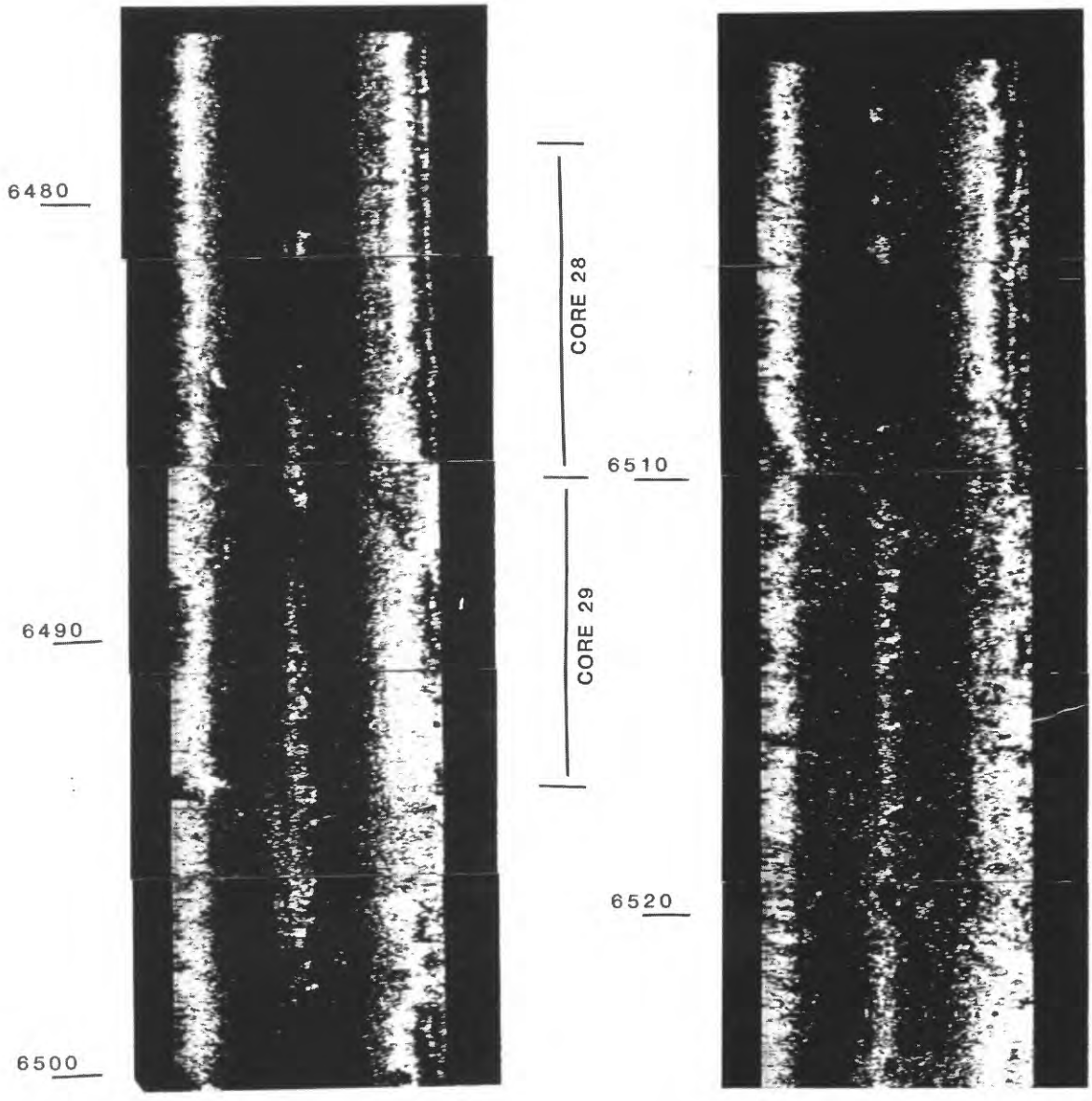
6480
6490
6500
CORE 28
CORE 29
6510
6520

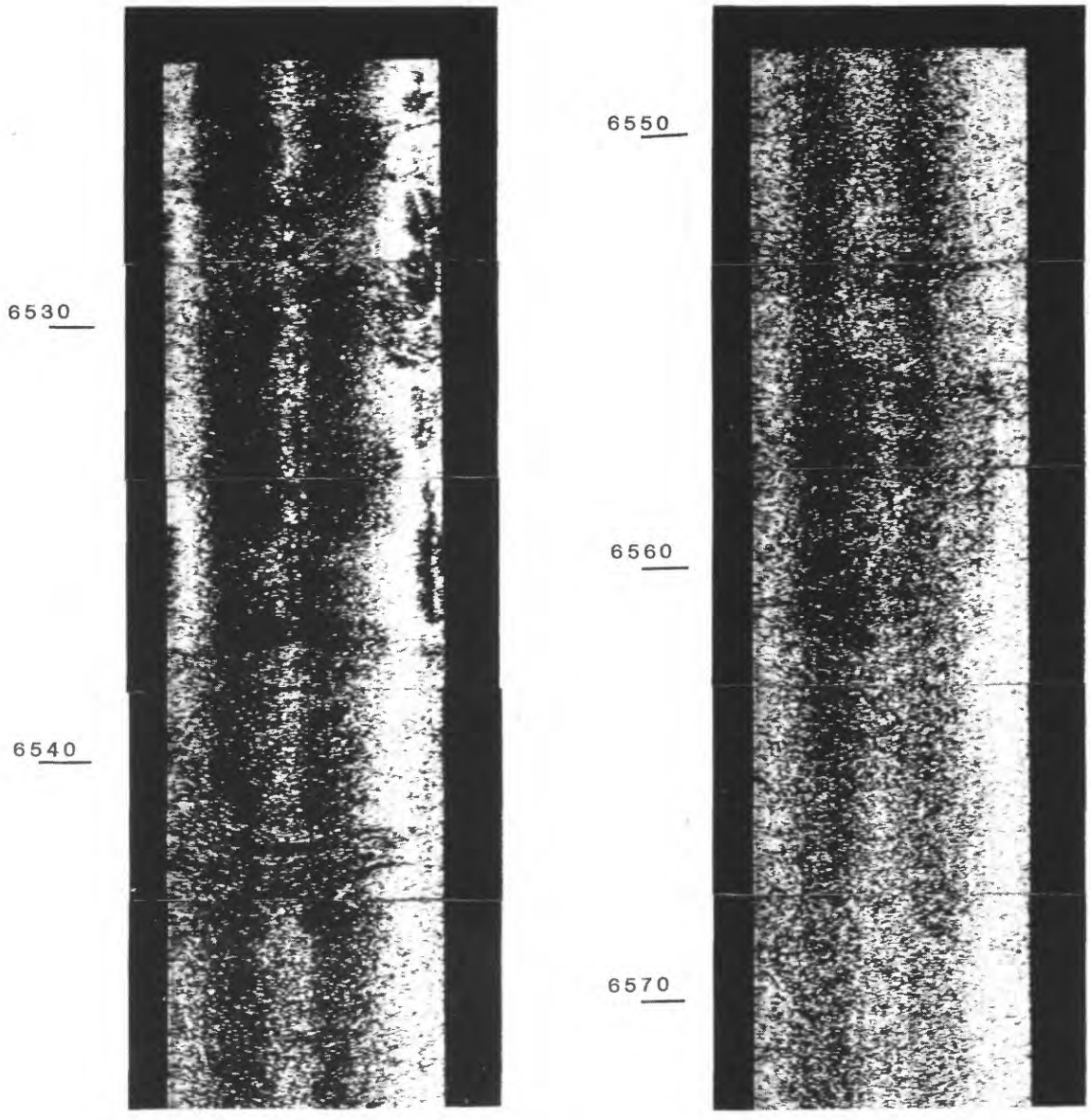
6530
6540
6550
6560
6570

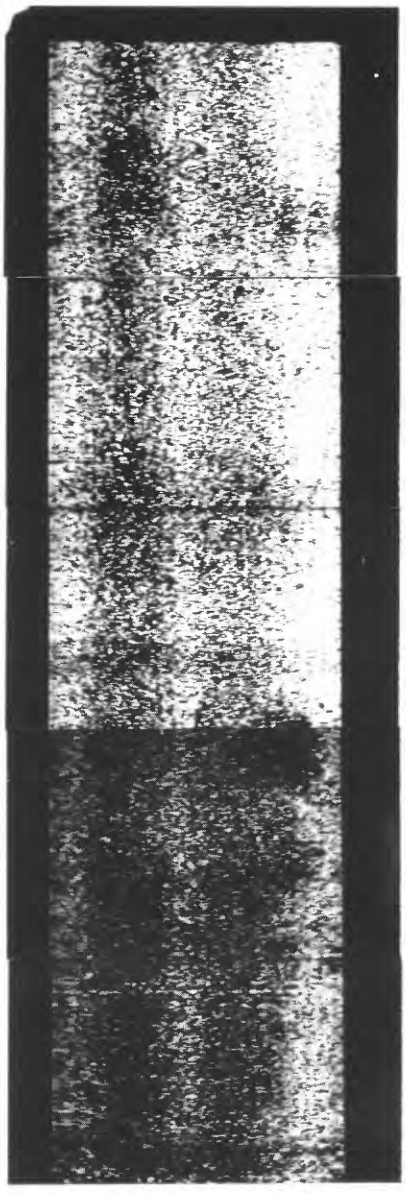
6580
6590

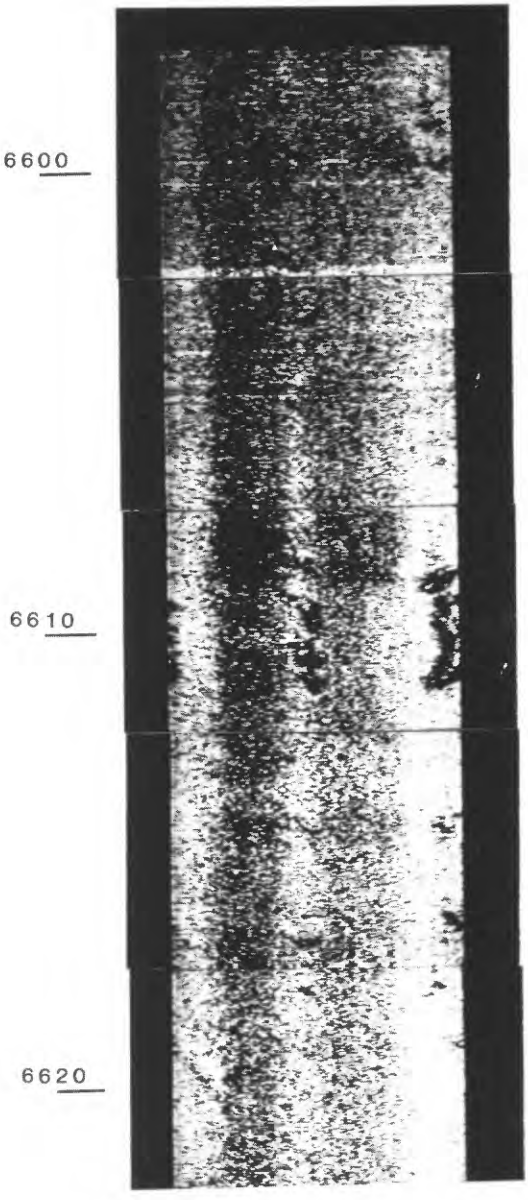
6600
6610
6620

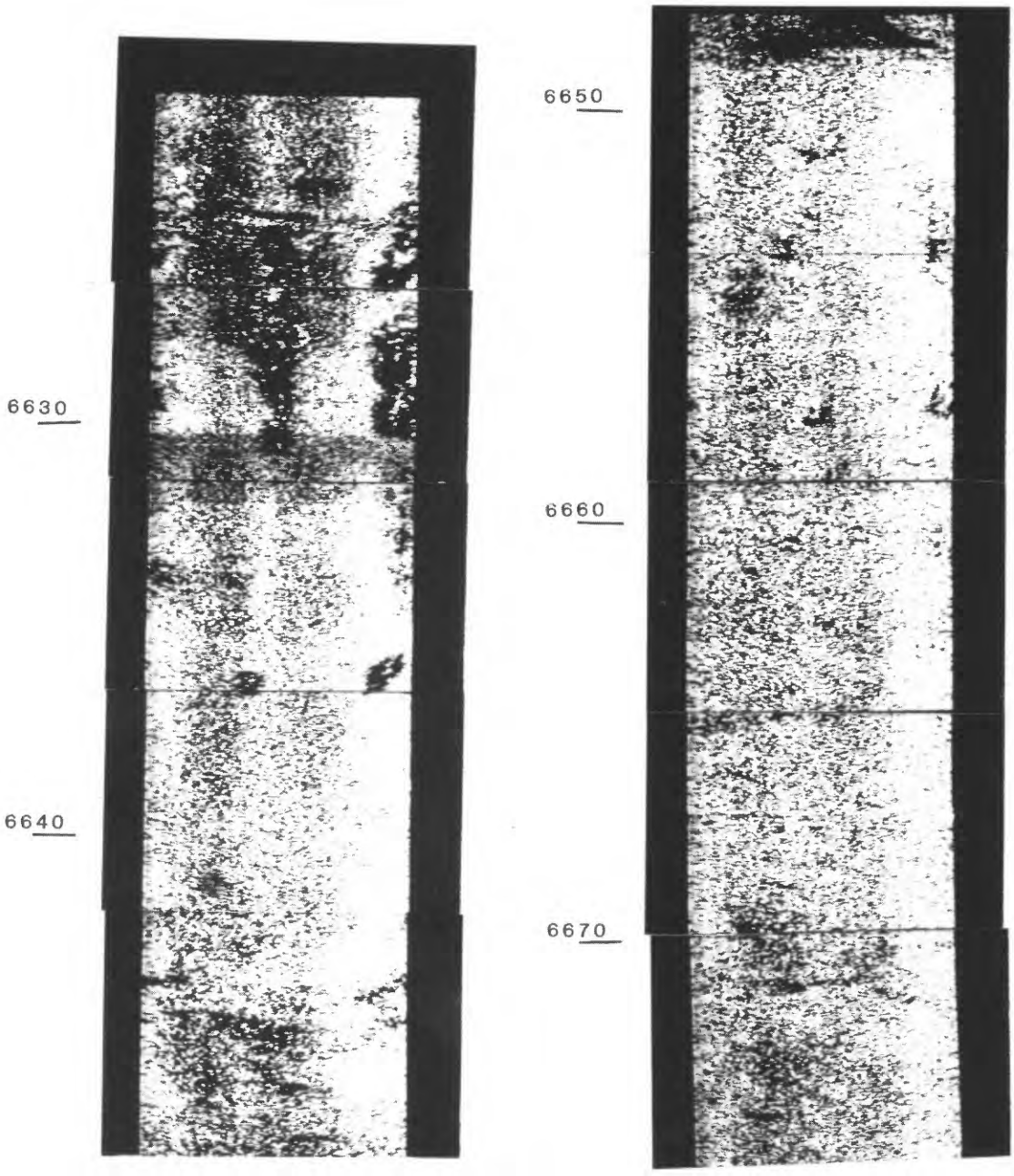
6630
6640
6650
6660
6670

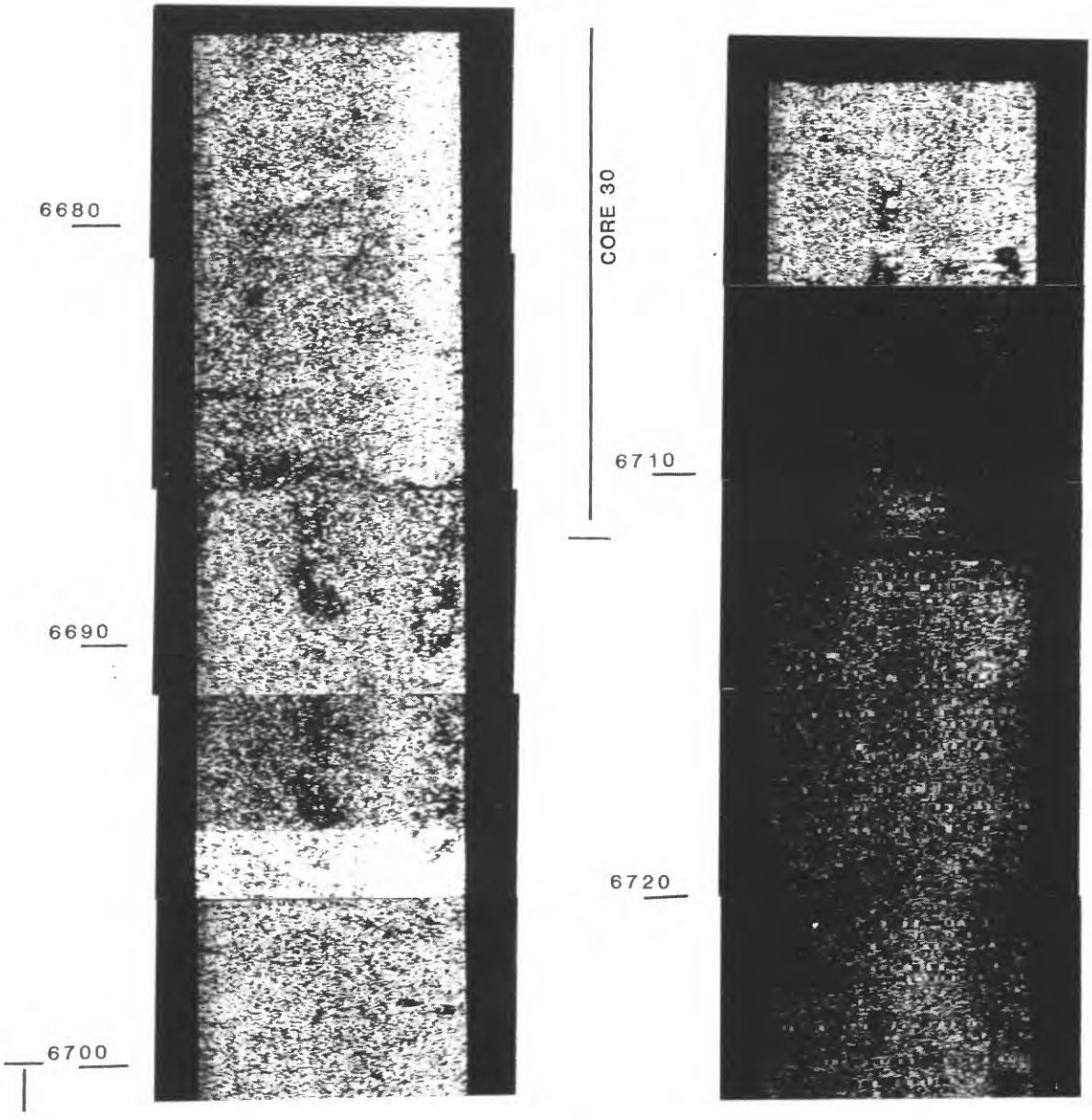
6680
6690
6700
CORE 30
6710
6720

APPENDIX B

TELEVIEWER LOG FROM THE 6-1/2 INCH SECTION OF THE HOLE

6-1/2 INCH HOLE

PRE-FRAC

POST-FRAC

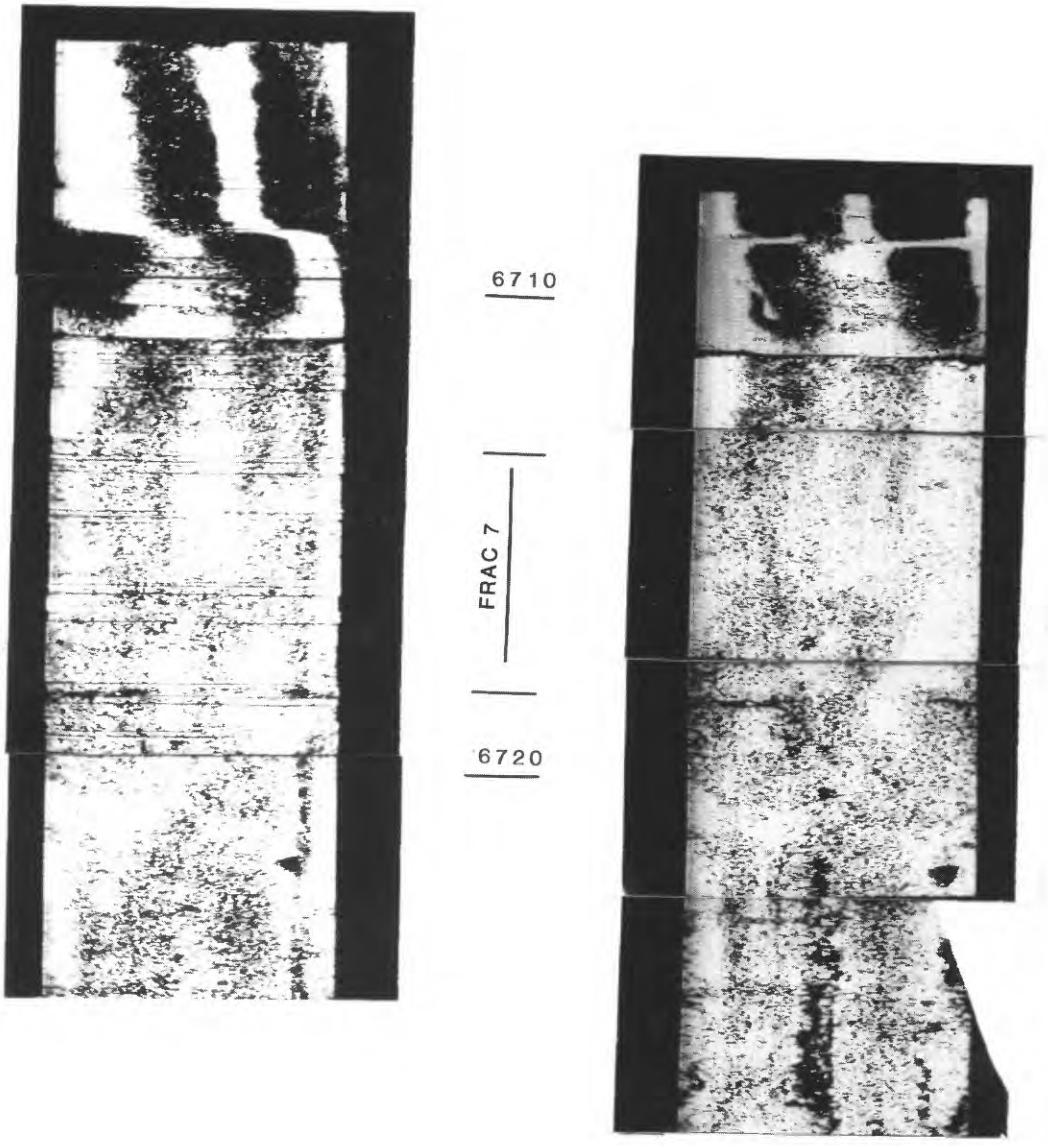

PRE-FRAC

POST-FRAC

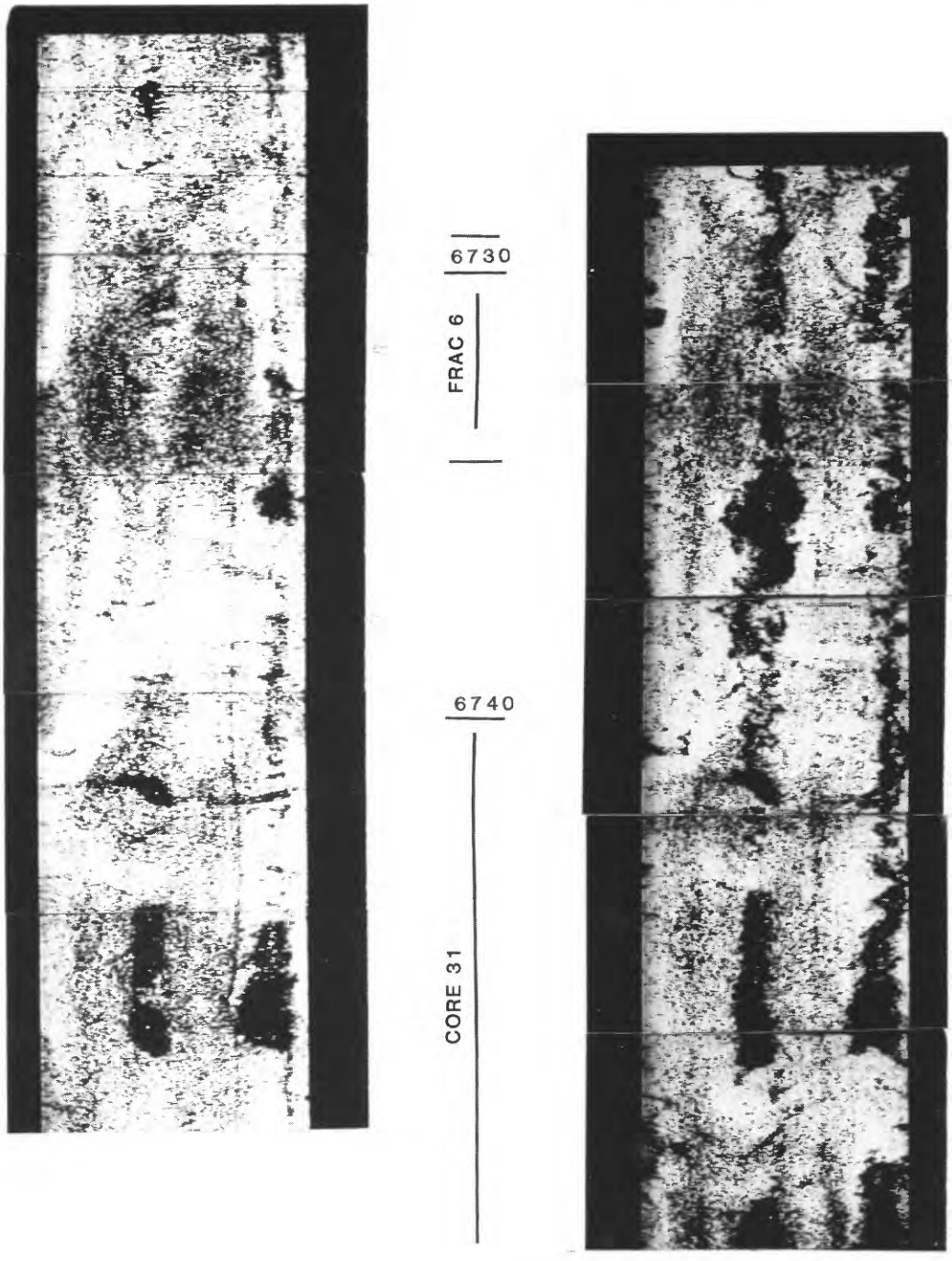

PRE-FRAC

POST-FRAC

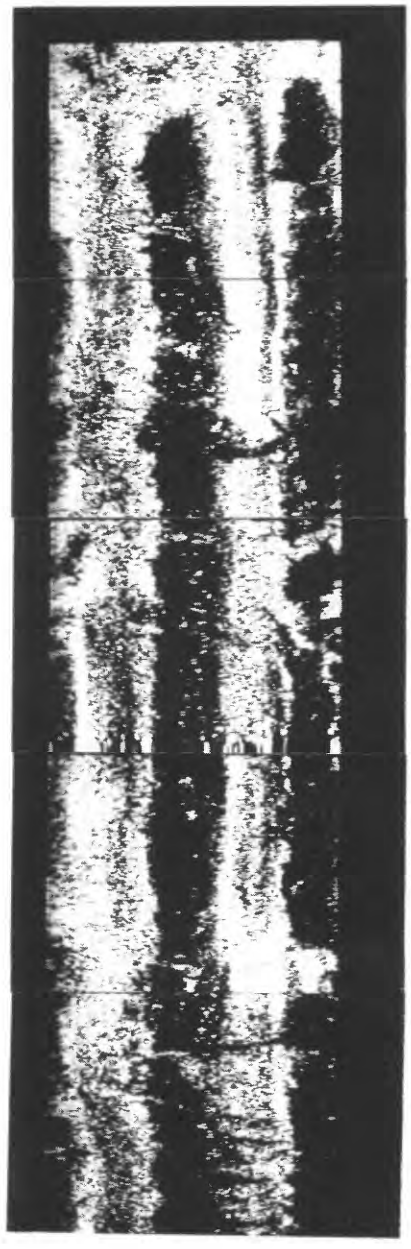

CORE 31

6760

6770

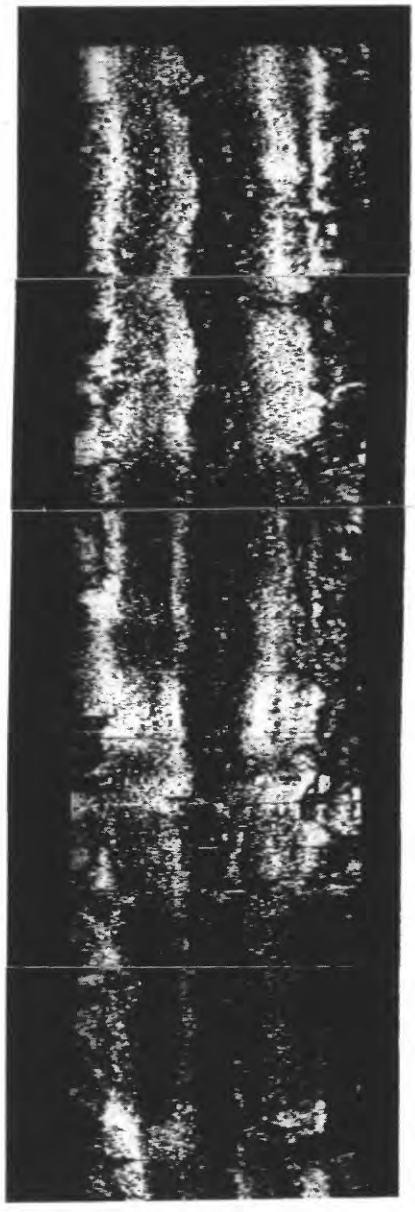

PRE-FRAC

POST-FRAC

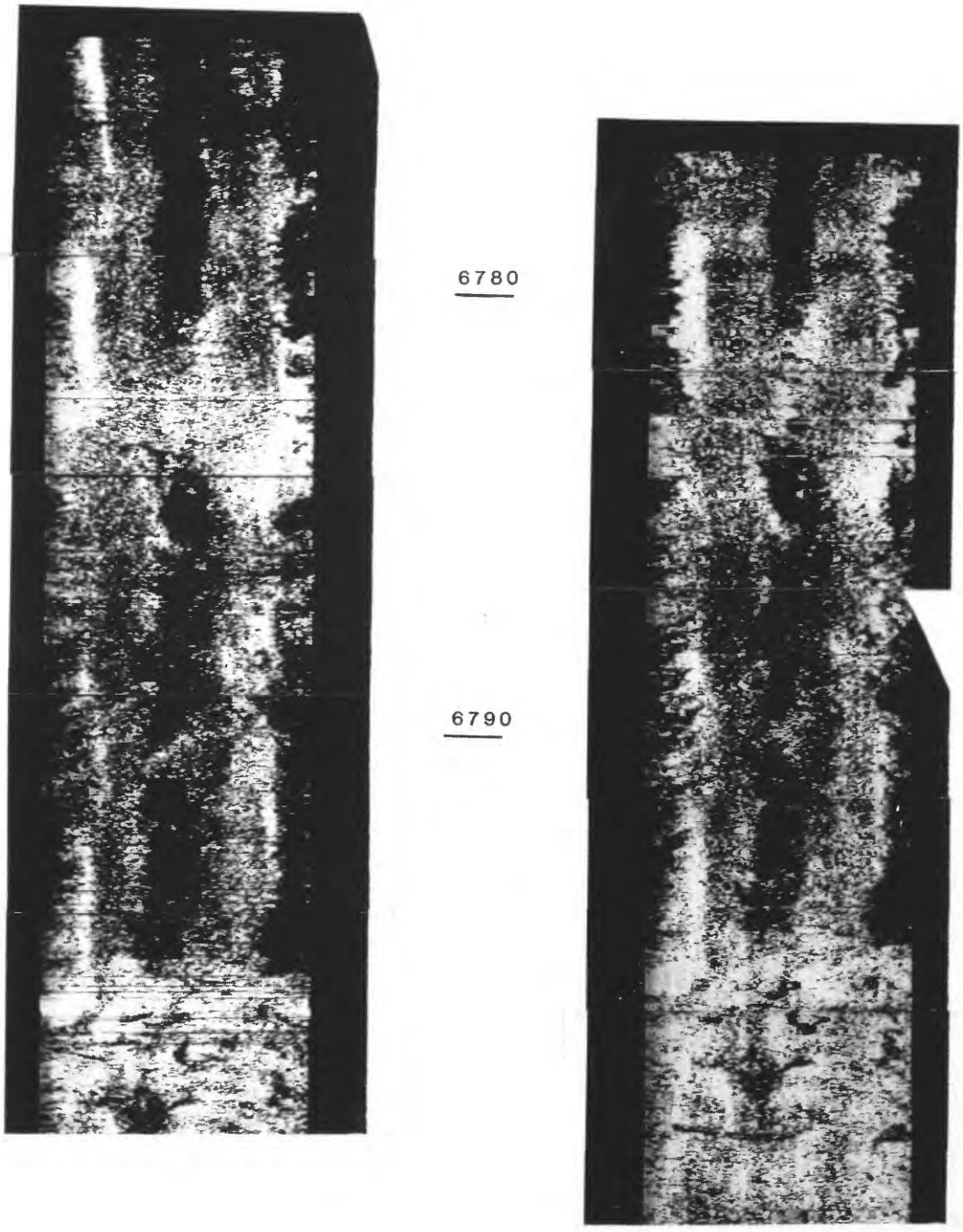

PRE-FRAC

POST-FRAC

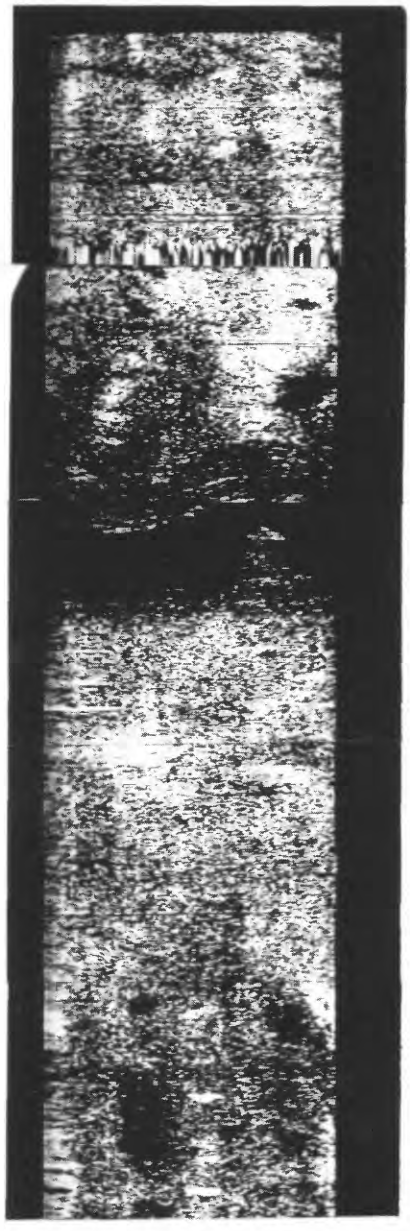

6805

CORE 32

6815

CORE 33

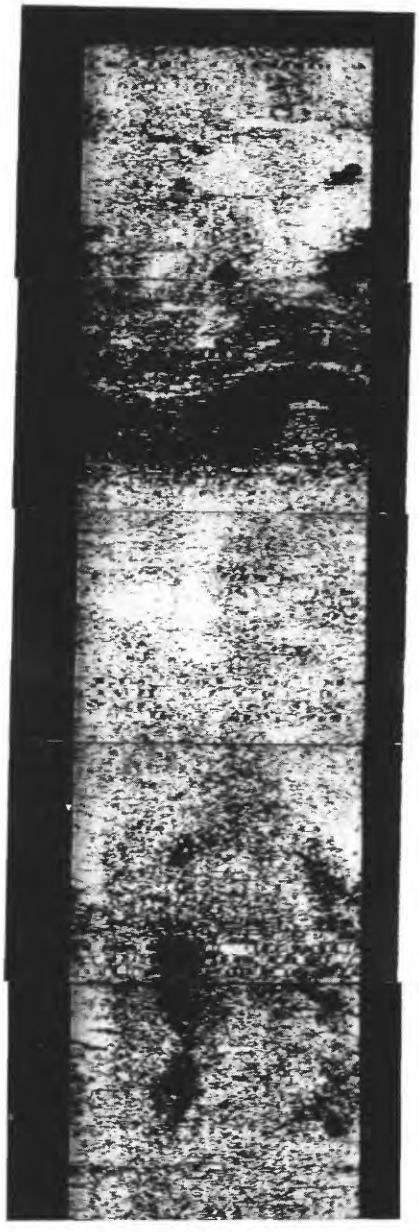

PRE-FRAC

POST-FRAC

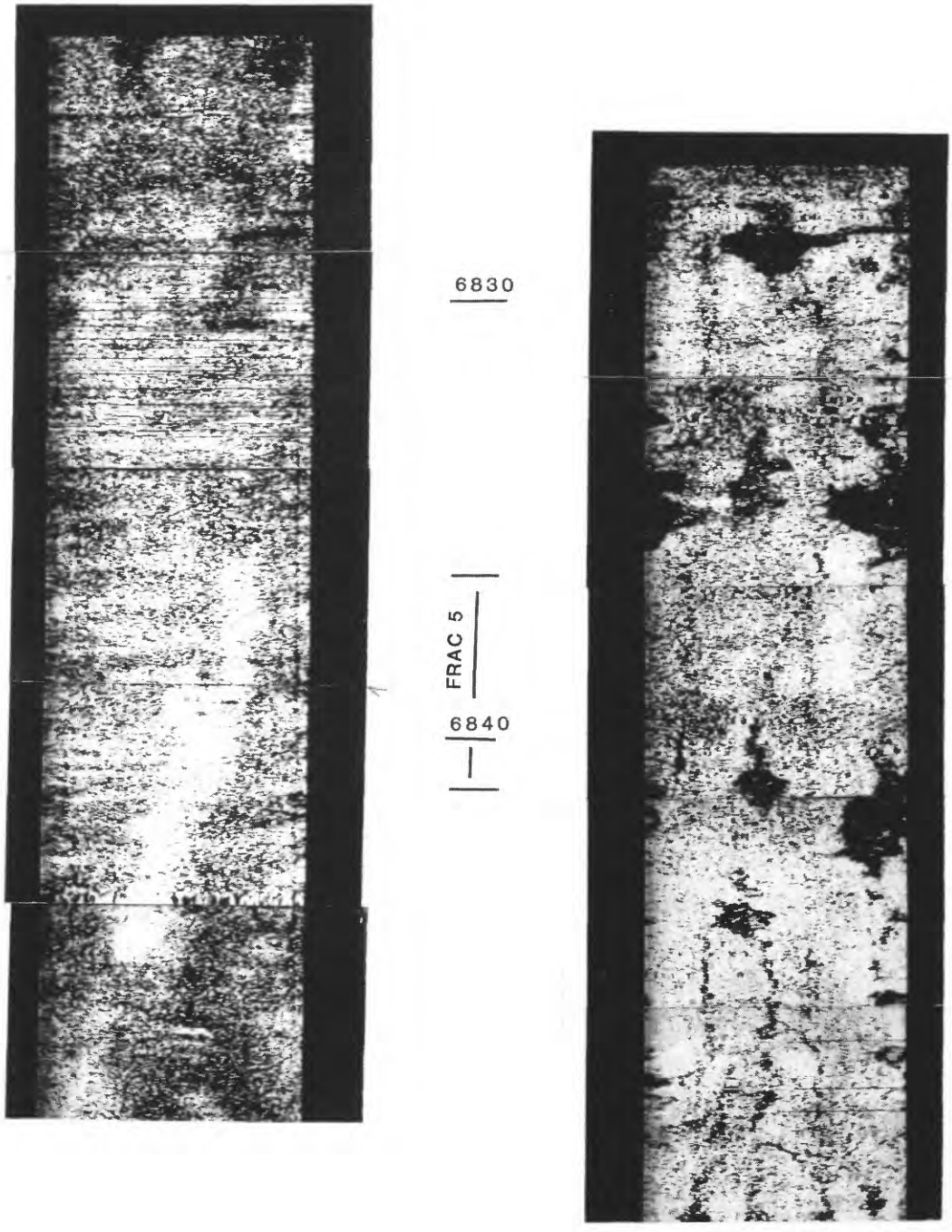

PRE-FRAC

POST-FRAC

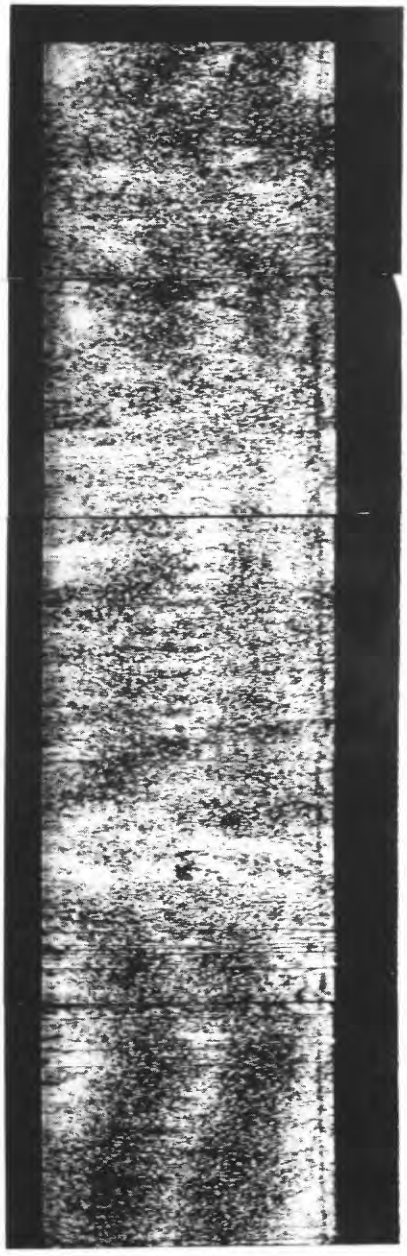

6855

FRAC 4

6865

PRE-FRAC

POST-FRAC

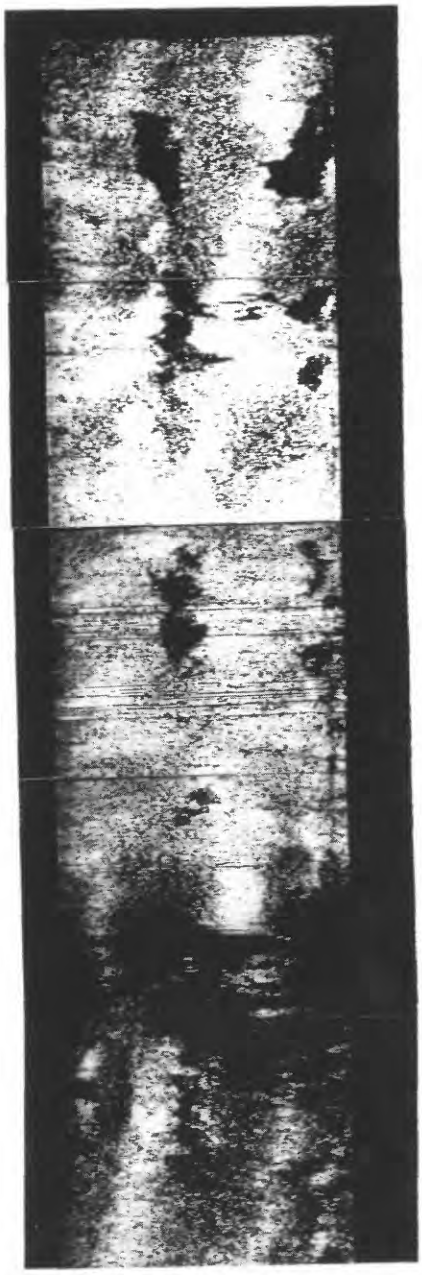

6880

6890

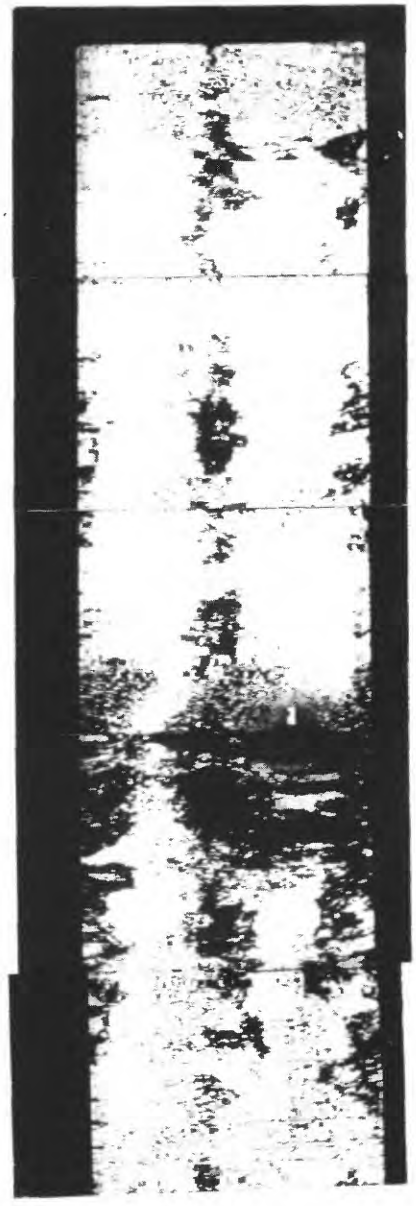

PRE-FRAC

POST-FRAC

6905

6915

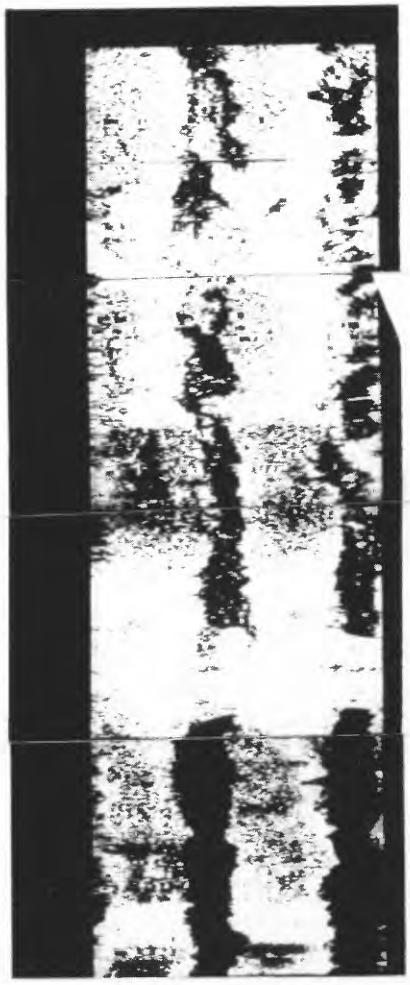

PRE-FRAC